Met Office

ESCAT soil moisture climatology

Forecasting R&D Technical Report No. 551

June 2011

Yaswant Pradhan, Malcolm Brooks, Roger Saunders

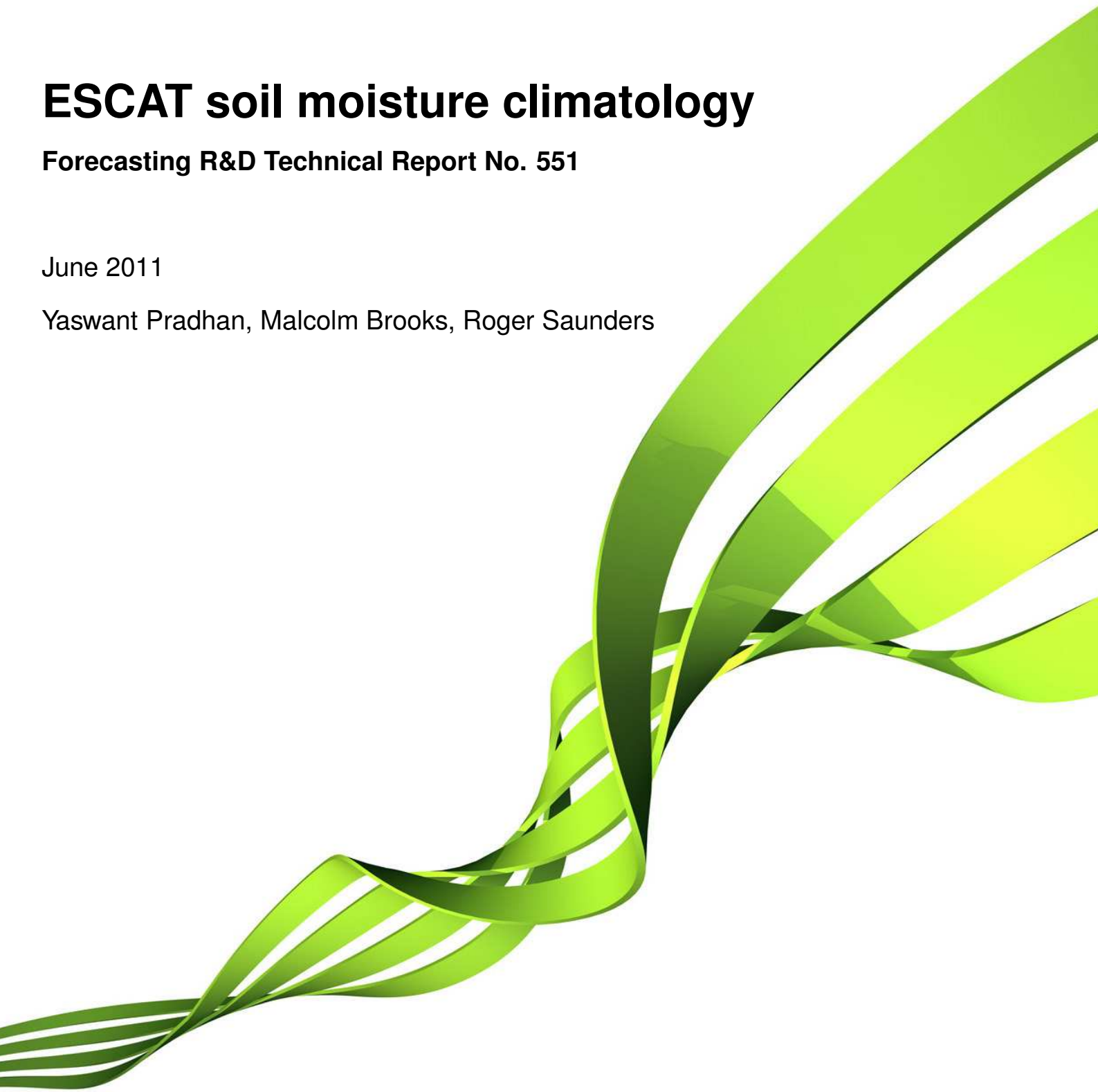

Document revision history

Version	Date	Changed by	Reason for change/Comments	Approval
0.1	Nov 2010	YP	First issue of the document	-
0.2	Jan 2011	YP	Included comments by RWS, MEB	-
0.3	Apr 2011	YP	Included SAM analysis for full 2010	-
1.0	Jun 2011	YP	Included comments by RWS, JE	JE

Contents

This page is intentionally left blank.

1 Introduction

Soil moisture is one of the key variables which control the exchange of water vapour and heat energy between the land surface and the atmosphere through evaporation and plant transpiration. It plays an important role in the production of precipitation. Large-scale dry or wet surface regions have been observed to impart positive feedback on subsequent precipitation patterns [8]. Simulations with numerical weather prediction models have shown that improved characterization of surface soil moisture, vegetation, and temperature can lead to significant forecast improvements [1].

Knowledge of soil moisture is also vital for downstream impact advice of trafficability (soil capacity to support military vehicles) in theatre. Trafficability is primarily a function of soil moisture content and soil type; therefore, observation of soil moisture is crucial for its analysis, forecast and verification.

This report describes a monthly climatology of surface and profile soil moisture record compiled using ESCAT (scatterometers onboard ERS-1 and ERS-2) level 2 soil moisture timeseries (1992-2007) generated at the Vienna University of Technology (TU-Wien). The first section explains the generation methods of global monthly climatology of Surface Soil Moisture (SSM at top 5cm) and Soil Water Index (SWI at top 1m). Secondly, a comparative study between the soil moisture climatology thus constructed and the Met Office soil moisture analysis in the Southern Asia model (SAM) during 2009-10 (when significant changes have occurred in the NWP suite) is carried out. Finally, the findings of the study are briefly described. The climatology maps of monthly mean and standard deviations of surface (0-5 cm) and profile (0-1m) soil moisture are depicted in Annex-3.

2 Soil moisture retrieval from ERS-1 and ERS-2 scatterometer

The dipole moment of water molecules causes orientational polarisation, resulting in high dielectric constant and hence high backscatter. At low microwave frequencies (1-10 GHz domain), the dielectric properties of soil and water are distinctly different. Therefore, scatterometers onboard earth observing satellites offer a relatively direct opportunity to measure soil moisture content in the soil surface layer. The European Remote-sensing Satellites (ERS-1 and ERS-2) were launched by the European Space Agency in 1991 and 1995, respectively. Both ERS satellites were built with a core payload of two specialised radars and an infrared imaging sensor. The two spacecraft were designed as identical twins except that ERS-2 carried the Global Ozone Monitoring Instrument (GOME) which was designed to monitor ozone levels in the atmosphere. The scatterometer onboard the ERS-1 and ERS-2 is part of the Active Microwave Instrument (AMI) consisting of synthetic aperture radar and a fan beam scatterometer operating in **C-band** (5.6 GHz) at **VV polarization**. The three scatterometer antennae generate radar beams looking sideways with respect to the satellite flight direction, at 45° (fore), 90° (mid), and 135° (aft), and at incidence angles ranging from 18° to 59° [2]. The three antennae beams continuously illuminate a 500 km wide swath, each measuring the radar backscatter over so-called *Cells*, which are approximately 50 km wide and spaced at 25 km from each other (for the Level 1 data). As a result the scatterometer provides three independent backscatter measurements

(a σ^0 triplet) at the nodes of a 25 km swath grid, taken practically simultaneously and at different viewing angles. ERS-1 had regularly acquired data during August 1991-May 1996. ERS-2 operated nominally between March 1996 and January 2001. Due to the failure of a gyroscope, soil moisture retrieval using ERS-2 scatterometer has not yet been possible between 2001 and 2003. ERS-2 lost its onboard data storage capability in June 2003 which limited the reception of its data to selected regions (North America, Europe, Northwest Africa, China and Australia) since May 2004.

2.1 TU-Wien Soil moisture retrieval method

ESCAT Level-2 soil moisture products were generated using the Water Retrieval Package (WARP) version-5.0 at the Vienna University of Technology (TU-Wien). The TU-Wien soil moisture retrieval method is a change detection approach, which accounts indirectly for surface roughness and land-cover (Figure 1). The following primary assumptions were made in the TU-Wien soil moisture retrieval method:

- Roughness and land-cover are temporally invariant at the scatterometer resolution. The measurement process suppresses local fluctuations of these parameters, due to the relatively high homogeneity of these measurables within the scatterometer footprint.
- Influences of vegetation phenology on σ^0 are identical from year to year.
- There exist distinct incidence angles θ_{dry} and θ_{wet}, where the backscattering coefficient is relatively stable despite seasonal changes in above ground vegetation biomass for dry and wet conditions, respectively.
- The relationship between soil moisture and σ^0 (expressed in dB) is linear [21].

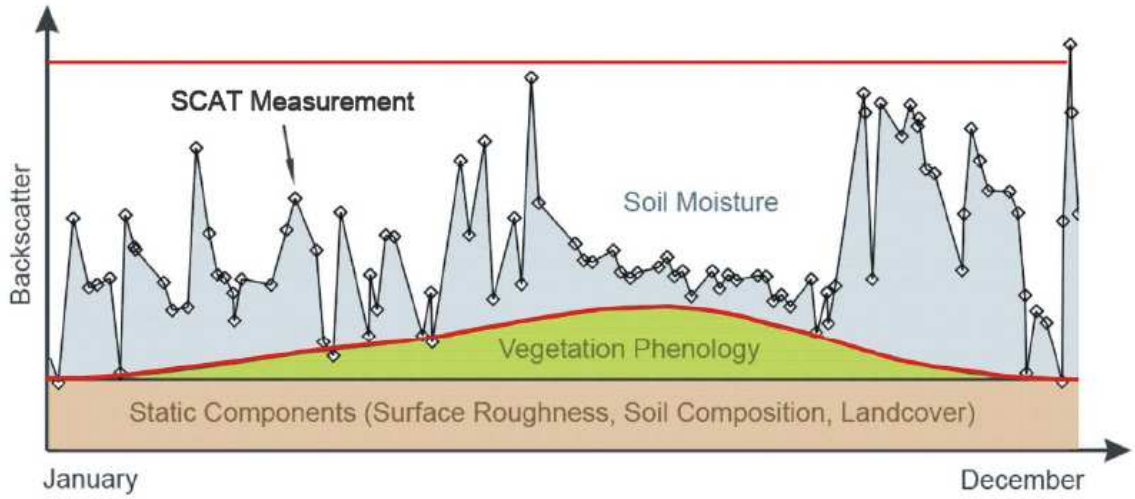

Figure 1: TU-Wien change detection approach for soil moisture retrieval using radar backscatter signal. Concept and figure courtesy of Wolfgang Wagner

2.1.1 Surface Soil Moisture (*SSM*)

The intensity of backscatter signal strongly varies with the incidence angle. In order to obtain soil moisture values, instantaneous backscatter measurements were normalised to a reference incidence angle of 40° and corrected for the seasonal influence of vegetation [2]. This was done by exploiting the multi-incidence angle viewing capabilities of the ERS scatterometers (Annex-1). The reference angle of 40° was found optimal for minimum extrapolation errors [23]. The normalised backscatter coefficients were then compared to equivalent existing dry and wet ERS backscatter references (θ_{dry} and θ_{wet}, respectively), also defined at 40°. As a result, time series of the topsoil (**<5 cm from surface**; scatterometer signals can penetrate only a few centimetres of the soil surface) moisture content were obtained by using the following formulation:

$$m_s(t) = \frac{\sigma^0(40,t) - \sigma^0_{dry}(40,t)}{\sigma^0_{wet}(40,t) - \sigma^0_{dry}(40,t)} \tag{1}$$

The backscattering coefficients for dry (σ^0_{dry}) and wet (σ^0_{wet}) conditions of soil surface were taken from a long-term global reference scattering parameter database created using ERS-1 and ERS-2 timeseries [2]. The retrieved surface soil moisture (*SSM*) m_s is a relative measure of the water content in the surface layer ranging between zero and one (or 0-100%). If σ^0_{dry} and σ^0_{wet} are respectively represented as a completely dry and a saturated soil surface, then m_s can be considered as the degree of saturation (i.e., the soil moisture content expressed in percent of porosity [11]). The scientific basis and algorithms for SSM retrieval using scatterometer data have been well documented in several publications [15, 16, 17, 26, 23, 25, 24].

2.1.2 Soil Water Index (*SWI*)

The retrieved SSM, being a topsoil signature, may change significantly within a few hours whose magnitude depends on the amount of rainfall, evaporation rate and the time lapse since the rainfall event. In many agro-meteorological applications, it is the soil moisture content at a certain depth is of more interest than the topsoil moisture. WARP-5 uses a simplified two-layer infiltration model [22] in which a) the water content in the surface layer is highly dynamic and attributed to precipitation, evaporation and surface runoff and b) the water content in the reservoir varies slowly because its rate of change is limited by the amount of water that can be exchanged with the surface layer and is fully explained by the past dynamics of the SSM. The Soil Water Index (SWI) for the **top 1m layer** thus estimated from the topsoil moisture content (m_s) using the following relationship:

$$SWI(t) = \frac{\sum_i m_s(t_i) \cdot e^{-\frac{t-t_i}{T}}}{\sum_i e^{-\frac{t-t_i}{T}}} \qquad for\ t_i \leq t \tag{2}$$

where, m_s is the surface soil moisture estimated from the ERS scatterometer at time t_i. The TU-Wien model integrates all measurements from a 100-day interval prior to the SWI sample time and weights the most recent measurements to contribute strongest to the respective SWI sample.

The SWI was calculated if at least one ERS Scatterometer measurement in the time interval $[t, t - T]$ and at least three measurements in the interval $[t, t - 5T]$ were available. The parameter T is the characteristic time length obtained from the maximum correlation between SWI and ground observations which equals 20 days for 0-100cm layer [23]. Like the SSM, the SWI is a trend indicator in relative units ranging between *wilting level* and *field capacity*. Although the model is quite simple, assuming a standardised soil neglecting different climatic condition throughout the year, the retrieved information is generally in good agreement with general climate regimes and gridded precipitation data [19].

Level-2 SSM and SWI products also include their noise, derived by error propagation of the backscatter noise covering instrument noise, speckle and residual azimuthal effects.

2.1.3 Validation of Level-2 *ESCAT* soil moisture products

Several studies in the past [16, 19] have found good agreement between ESCAT soil moisture product and ground based soil moisture observations. Naeimi and others [16] compared the ERS scatterometer derived surface soil moisture with *in situ* measurements at 5 cm of Fractional Water Index (FWI[1]) from the Oklahoma Mesonet, for the three year period (2004-2006) and found high correlations between the derived soil wetness and *in situ* FWI measurements. They also found high correlation between the scatterometer derived soil wetness and ERA-Interim reanalysis soil moisture data. In another study, Scipal [19] compared ERS derived volumetric soil moisture (using an empirical relationship between the volumetric soil moisture and the profile soil water index) with *in situ* observations from China, Russia, Ukraine, Illinois and India. He reported an accuracy of around $0.05 - 0.07\, m^3/m^3$ between the ERS derived volumetric soil moisture and *in situ* measurements. Several other studies indicated the ESCAT profile soil moisture dataset (SWI) to reflect trends in precipitation [10, 26], modelled soil moisture [7, 13, 18], *in situ* soil moisture [4] and runoff [5, 20].

2.2 Construction of monthly mean climatology

Level-2 global SSM and SWI timeseries data were obtained from TU-Wien secure ftp server[2] for the entire ERS-1 and ERS-2 operation period (1992-2007) with an exceptional data gap between January 2001 and August 2003 due to failure of several on-board gyro systems. The data were stored in a timeseries format within a predefined irregular 12.5km grid, also known as Discrete Global Grid (DGG[3]).

[1] Fractional Water Index is a dimensionless quantity that varies from zero (very dry soils) to one (very wet soils). There is a non-linear relationship between FWI and soil moisture which strongly depends on soil texture.

[2] ftp.ipf.tuwien.ac.at

[3] DGG is an adapted sinusoidal grid using an ellipsoid based on the Goddard Earth Model (GEM-6). The grid is defined such that the spacing is approximately 12.5 km. The grid consists of 3,264,391 points out of which 839,826 points are defined over land.

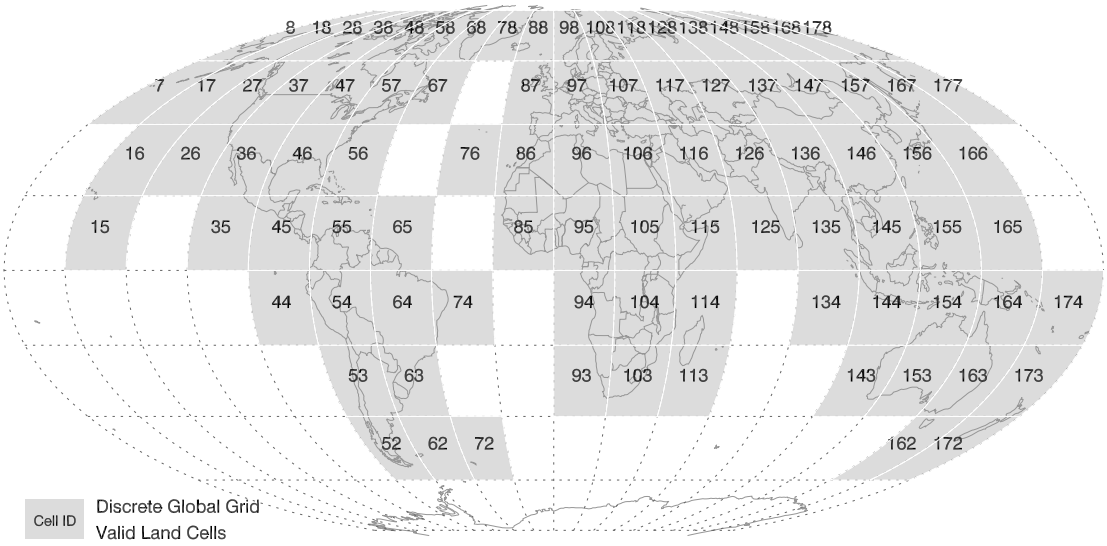

Figure 2: ESCAT cells over land; each cell contains sub-sample coordinates, spaced ~12.5km apart, from a pre-defined sinusoidal Discrete Global Grid.

The DGG was split into 18×10 grid cells (Figure 2) from which each grid point could be identified by a unique Grid Point Index (GPI) corresponding to fixed geographic location on the Earth. It is worth to mention that given the present 50 km resolution of the ERS data, the 12.5 km grid spacing implies an oversampling of the actual observation. The monthly climatology metrics were calculated for each valid grid point using the set of equations defined in Table 1. For each grid point, all valid samples were accumulated for specific months. At least 3 valid samples were required for the computation of the monthly statistics. The monthly SSM and SWI climatology thus created using the ~15 years ERS-1/2 scatterometer data were stored in Network Common Data Format (netCDF[4]). Monthly climatology maps of average SSM and SWI are depicted in Annex-3 of this report.

[4]NetCDF (network Common Data Form) is a set of software libraries and machine-independent data formats that support the creation, access, and sharing of array-oriented scientific data. Further details available at UCAR website http://www.unidata.ucar.edu/software/netcdf

Table 1: Monthly climatology metrics. In the formula y represents *SSM* (and noise) or *SWI* (and noise) and the subscripts m and i correspond to month number and observation index, respectively.

Metric	Formulae	Definition
Average	$\frac{1}{N}\sum_{i=1}^{N} y_{m,i} \quad where\, N > 3,\ m = 1...12$	Arithmetic mean of the variable y for a specific month m
Standard deviation	$\sqrt{\frac{1}{N}\sum_{i=1}^{N} (y_{m,i} - \overline{y_m})^2} \quad where\, N > 3$	Sample standard deviation of the variable y for a specific month m.
Minimum	$\min(y_i) \quad where\, 0 \leq y_i \leq 100$	Minimum value of the variable y for a specific month m
Maximum	$\max(y_i) \quad where\, 0 \leq y_i \leq 100$	Maximum value of the variable y for a specific month m.
Number of observations	$\sum i_m \quad where\, 0 \leq y_{m,i} \leq 100$	Total number of valid observation used in climatology metrics for a specific month m.

2.3 Known retrieval problems

The TU-Wien method can retrieve the temporal variations accurately, although the absolute level of soil moisture can be biased in certain regions (W. Wagner, pers. comm.). Biased estimates were reportedly observed in extreme climates such as deserts (see next paragraph) and arctic regions. Azimuthal artefacts are known to occur mainly in mountainous and sand desert regions. The azimuthal viewing geometry of the ERS scatterometer was not taken into account in the retrieval method. Furthermore, retrieval of soil moisture is not possible under snow and frozen soil conditions or areas with highly undulated terrains, and is erroneous in open water surfaces.

During the development of ERS long-term scattering parameter database, the derived $\sigma^0_{wet}(40)$ was found to be too low in some arid regions due to the lack of saturated conditions during the entire observation period. In such cases, an empirical bias-correction factor based on sensitivity was applied to $\sigma^0_{wet}(40)$. The locations for which this wet correction was applied were determined by using an external climatology dataset [12]. Surface Soil Moisture (SSM) is very sensitive to rainfall events. WARP-5.0 did not have a suitable rainfall tracking method. However, the derived products have a reserved flag for future processing. Secondly, accurate retrieval of SSM over dense forest is challenging especially where the fraction of dense vegetation is larger than the scatterometer footprint. Nevertheless, the Level-2 timeseries record retained the retrieved SSM over all types of land surfaces excluding ice cover. The Level-2 products used in this report came with suitable flags to identify *Snow Cover probability, Frozen Soil probability, Inundation/Wetland fraction* and *Topographic complexity*; however, did not have any information on the vegetation/land-cover (see Figure 3 for an example of the ASCAT product with suitable vegetation flag). Therefore, it is recommended to use a dynamic land cover mask in conjunction with the climatology products in order to address the retrieval

problem over dense tropical forests. The available quality flag indicators are currently provided as separate binary files. A suitable approach to associate all quality flags including vegetation index will be implemented in the future release of the climatology dataset.

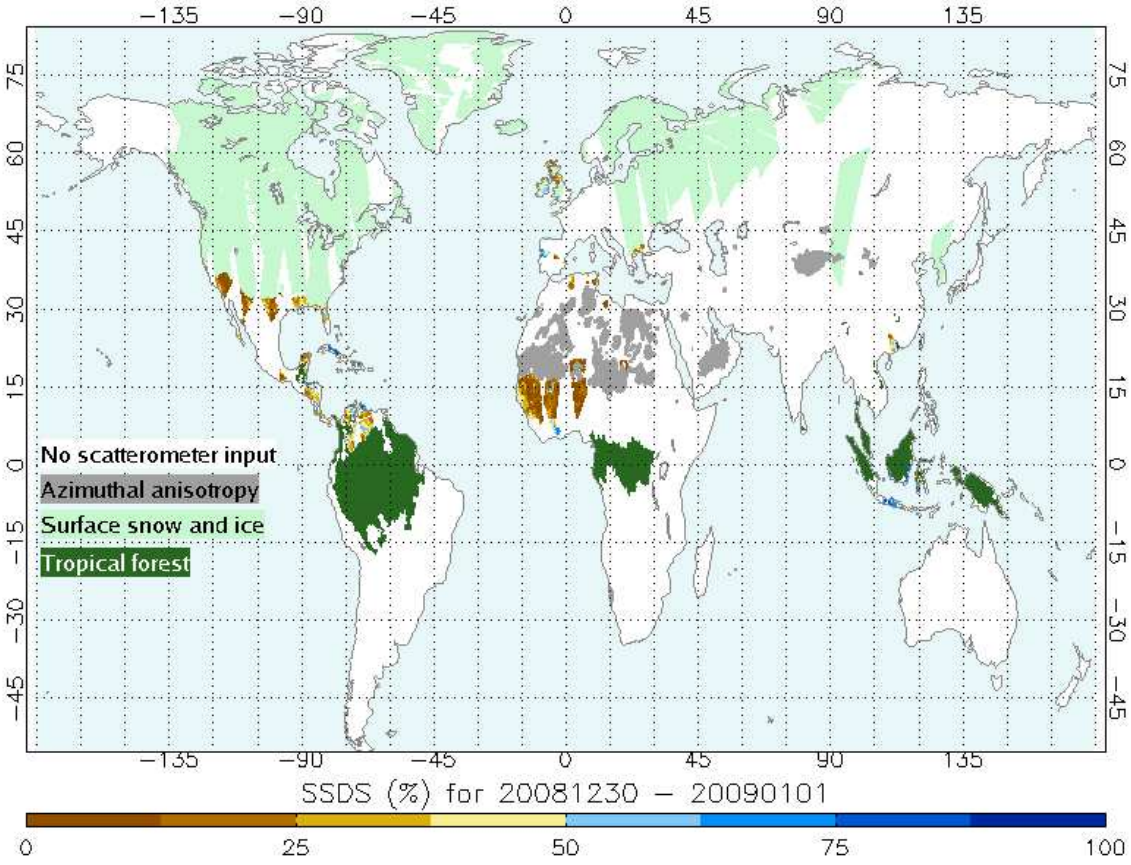

Figure 3: An example of useful flags implemented in Advanced SCATterometer (ASCAT on-board MetOp) soil wetness index data (figure courtesy of TU-Wien). Note that the tropical forest regions, flagged in green colour, are not implemented in the current version of ESCAT soil moisture products.

3 Model comparison

In this section we present results from a preliminary comparison of Met Office soil moisture analyses with the ESCAT soil moisture monthly climatology for 2009-2010 period, over the Southern Asia Crisis Area Model (SAM) domain (Figure 4).

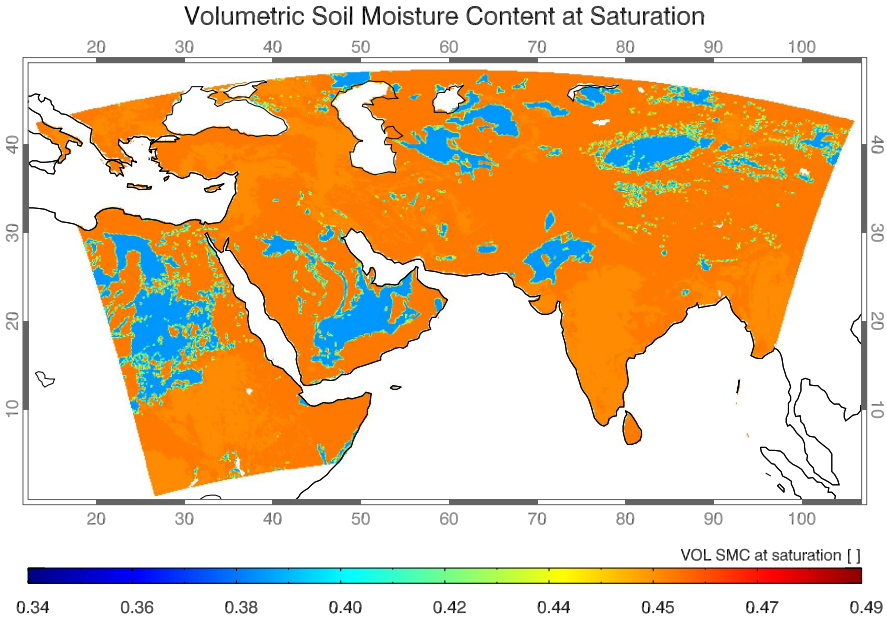

Figure 4: Southern Asia crisis area model (SAM) domain showing the volumetric soil moisture at saturation from latest (PS25) ancillary file qparam.soil.pp.

During the period 2009-2010, several changes have been made to the Met Office NWP system (Table 2). The most important changes with respect to the soil moisture analysis occurred in parallel suites (PS) 23 and 24 in March and July 2010, respectively.

Table 2: Changes to the Met Office NWP system (SAM specific) during 2009-2010 period.

PS	Date	Change
21	Jul 2009	Migration to IBM supercomputer.
22	Nov 2009	Upgrade SURF and STASH changes for NEON.
23	Mar 2010	⇒ Upgrade to 70 levels and 12 km ⇒ MOSES-PDM hydrology and new river flow model diagnostics in UM-7.4 ⇒ van Genuchten hydrology with HWSD soils
24	Jul 2010	⇒ Assimilation of ASCAT soil wetness ⇒ Modification to snow scheme

3.1 Operational UM Soil Moisture

The Met Office global Unified Model (UM) soil moisture analysis scheme uses observations of screen temperature and humidity. Recently, a computationally cheap nudging scheme to assimilate volumetric surface soil moisture from the Advanced Scatterometer (ASCAT) on-board Meteorological Operational (MetOp) satellite has been introduced in July 2010 [6]. Screen height (1.5 meters) observations of temperature and humidity are used to diagnose errors in the model soil moisture and the model soil moisture is nudged towards reality. The ASCAT has a similar heritage to the ERS scatterometers in terms of antenna technology and soil moisture retrieval method. However, the ASCAT instrument has two sets of antennae, extended incidence angle range (25°-65°), better radiometric performance and stability, better coverage (~3 times greater than that of ERS) and higher spatial resolution of 35km compared to ERS scatterometers [2]. Various suitable methods to convert level-2 ASCAT surface soil wetness (similar to ESCAT) to surface volumetric soil moisture, prior to assimilation, can be found elsewhere [6].

The UM uses the Met Office Surface Exchange Scheme (MOSES-2) for land surface process parametrisation [9]. The soil is discretised into four layers of thickness (Table 3). In this study, the analysed soil moisture content (SMC in kg/m^2) in the top three layers were converted to relative units in order to be comparable with ESCAT SSM and SWI climatologies.

Table 3: UM soil moisture content pseudo levels

Level	Range [top - bottom]	Thickness (dz)
1	surface - 10cm	10 cm
2	10 cm - 35cm	25 cm
3	35 cm - 1 m	65 cm
4	1 m - 3 m	200 cm

3.1.1 Conversion of model SMC to ESCAT equivalent soil moisture index

As described earlier, the ESCAT SSM (top 5 cm) and SWI (top 1 m) climatology data are expressed in normalised units (%) - with 0 meaning completely dry and 100 meaning saturation level. We applied a normalisation procedure to SAM soil moisture fields in order for it to be comparable with ESCAT climatology.

The model SMC in a layer was converted to Volumetric Soil Moisture Content (θ in kg/m^3) and then normalised with Volumetric Soil Moisture Content at Saturation (θ_s) to obtain model soil moisture index in relative units (%):

$$\Theta_z = \frac{\left[\frac{SMC_z}{0.01 \star dz}\right]}{\theta_s . \rho_w} \tag{3}$$

where, θ_s was taken from the latest ancillary file (Figure 4). The top level is essentially equivalent to the ESCAT SSM. The Θ values at the top three levels were weight-averaged in order to obtain the

moisture index for the top 1m (equivalent to ESACT SWI):

$$\hat{\Theta} = \sum_{z=1}^{3} w_z \cdot \Theta_z \tag{4}$$

where, the prescribed weights were $w = [0.1, 0.25, 0.65]$. SAM analyses (valid at 0Z) for 1st, 5th, 8th, 12th, 15th, 18th, 22nd, 25th and 28th dates of each month in 2009 and 2010 were used in the preparation of model monthly mean soil moisture data.

3.2 Climatology versus model analysis

3.2.1 Average soil moisture at top level (0-5cm, 0-10cm)

The spatial distribution of soil moisture in the Southern Asia domain exhibited strong seasonality mostly related to the Indian monsoon seasons. Figure 5 shows the spatial distribution of surface soil moisture climatology and analysed monthly means in 2009 and 2010 for March, June, September and December. Model analyses were relatively wetter compared to the climatology during winter months in higher latitudes (>30°N).

Following the model upgrades in March 2010, a better representation of the Taklimakan desert (in northwest China) and a significant reduction in patchiness of the analysed fields over the arid regions in North Africa and Middle East were generally observed. Dharssi et al. [6] have shown some positive impacts on NWP forecast skill in the tropics following ASCAT soil wetness data assimilation. Figure 6 shows that both climatology and model analyses captured the bimodal nature of soil moisture distribution in the SAM domain during the Indian summer monsoon period (June to September). In general, model analyses appeared to be wetter than the climatology, and 2009 appeared to be drier compared to 2010.

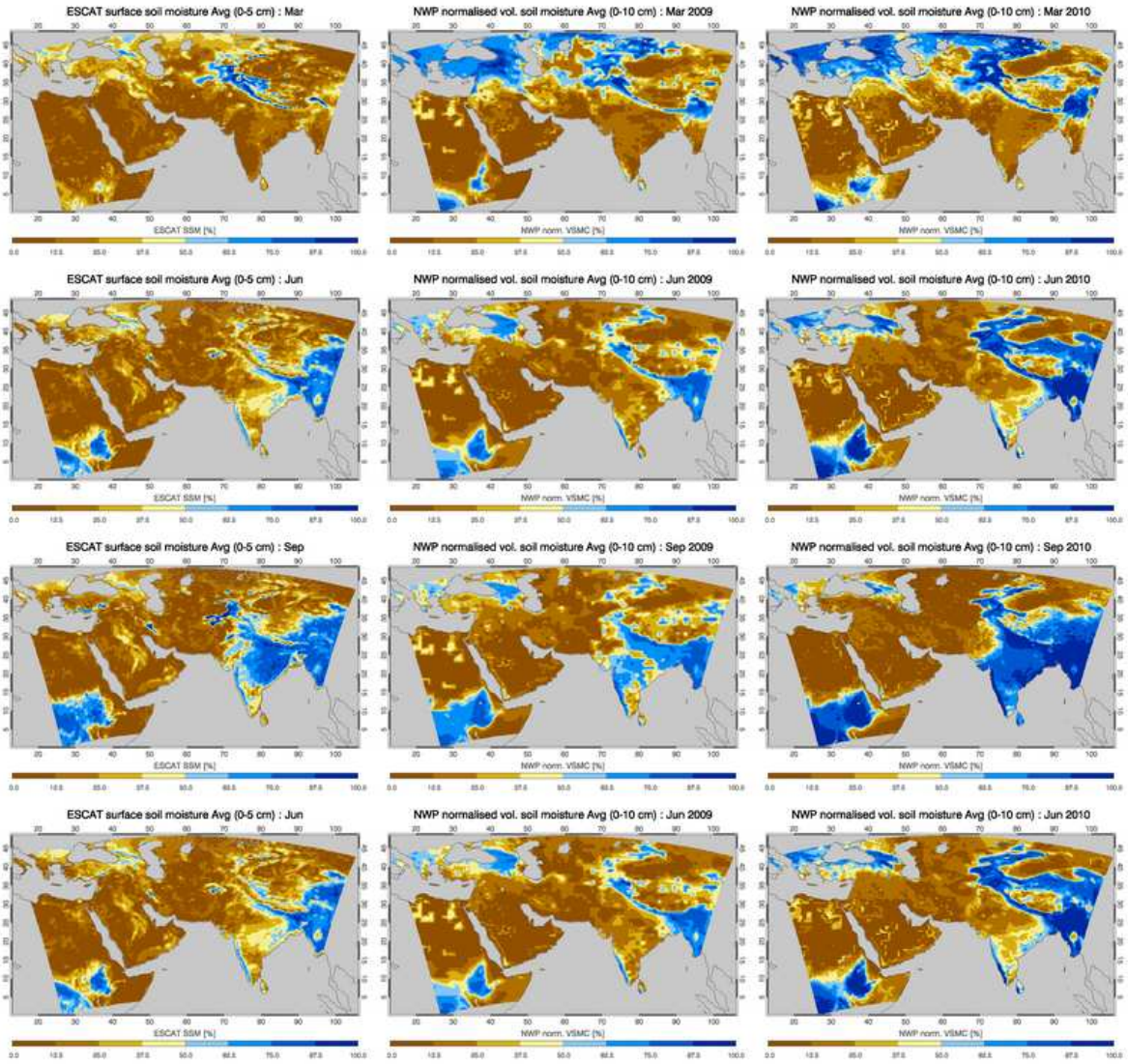

Figure 5: Four months (Mar, Jun, Sep, Dec, starting from top row) surface soil moisture maps climatology (left panel), model (SAM) analyses for 2009 (middle panel) and 2010 (right panel). The colour codes range from dark brown (0%) to dark blue (100%) indicating the driest and the wettest/saturated regions, respectively.

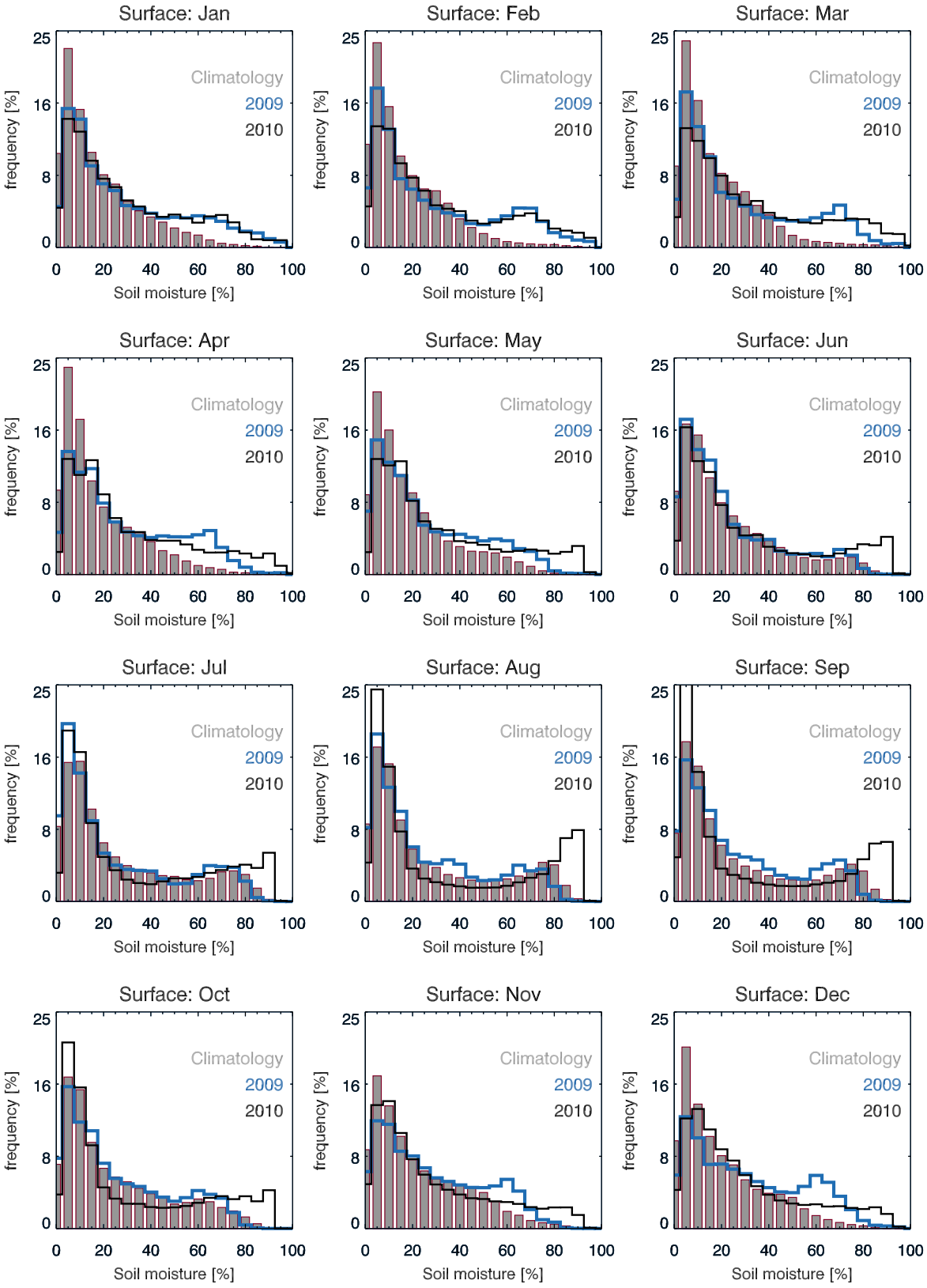

Figure 6: Monthly distribution of soil moisture climatology and model analyses (for 2009-2010) at near-surface level.

3.2.2 Average soil moisture at top 1m

Spatial distribution of monthly profile soil moisture climatology (at the top 1 metre) did not exhibit significant difference compared to the soil moisture climatology at surface layer (top 5cm). However, the distribution of column integrated monthly averages of UM soil moisture analyses$\hat{\Theta}$ (for 2009-2010) were significantly different from the ESCAT climatology at top 1 metre (Figure 7). The UM analysed field was generally wetter than ESCAT climatology for the top 1 metre layer over the SAM domain. In principle this may indicate the anomalous events during a particular years; however, the distribution patterns of UM deep soil moisture for 2009 and 2010 had similar differences to ESCAT climatology with maximum offsets during northern hemisphere winter and spring implying a better parametrisation may be required to improve the ESCAT profile soil moisture retrievals. It is understood that the scatterometer soil moisture represents the precipitation events better that the deep soil moisture. In a regional study, the ESCAT SWI was reported to follow precipitation events better than the *in situ* soil moisture data over China [27]. In the same study the authors noticed a rapid reduction of the ESCAT profile soil moisture (SWI) with precipitation (after the rainy season) despite the high level (close to saturation) of moisture content in the deep soil layers as observed from the *in situ* measurements. Considering the simple exponential nature of the ESCAT SWI algorithm and its strong connection with the precipitation events, extreme caution should be taken while comparing SWI data directly with results from sophisticated numerical models such as the UM. Nevertheless, this preliminary study suggests that a further investigation of the UM soil moisture analysis, specifically in the deep layers, is necessary to fully understand the associated uncertainties.

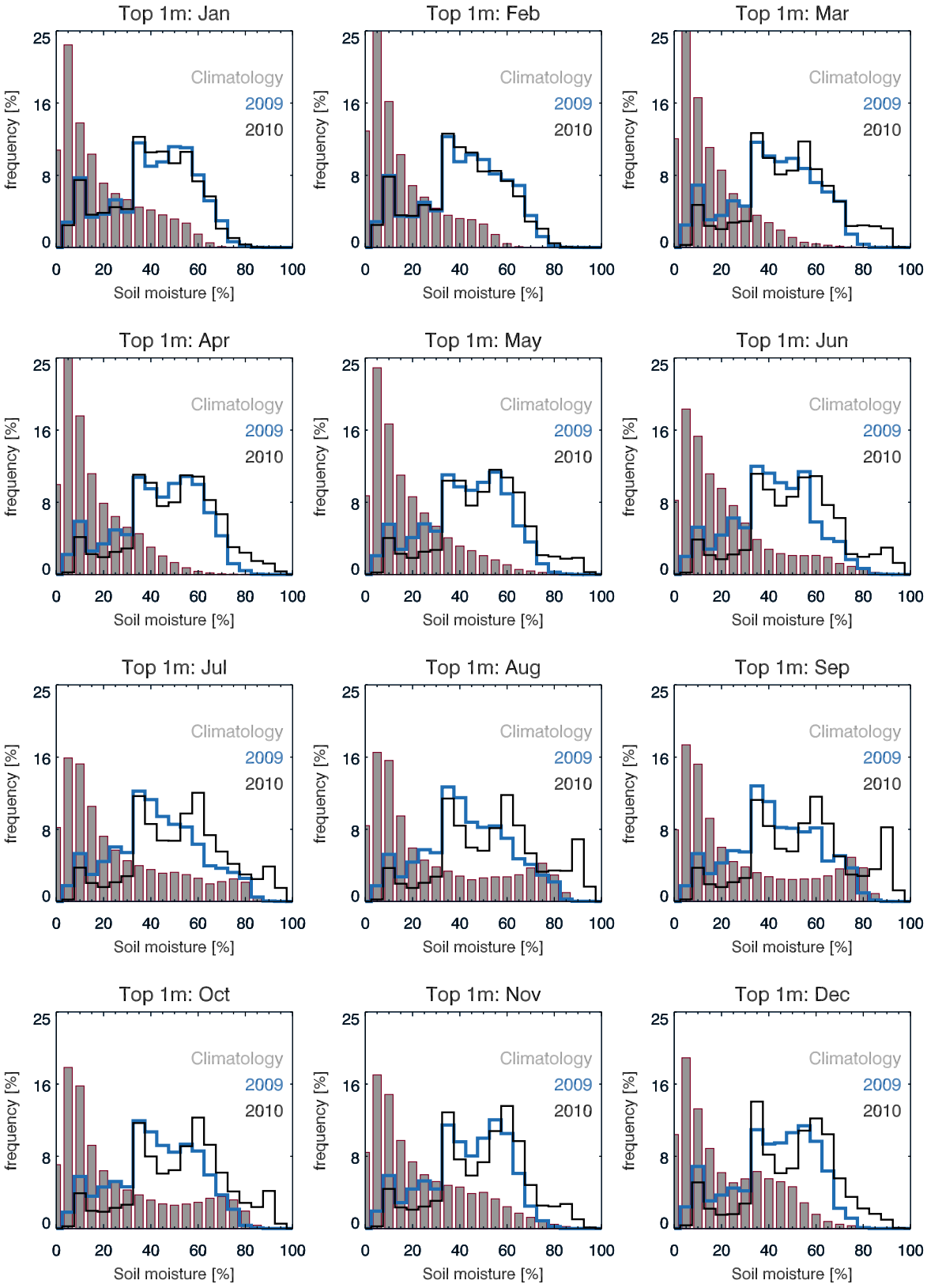

Figure 7: Monthly distribution of soil moisture climatology and model analyses (for 2009-2010) at top 1m level.

3.2.3 Timeseries analysis

Figure 8 shows the time evolution of soil moisture analysis against ESCAT climatology, over the whole SAM domain. A distinct seasonal cycle peaking around the Indian summer monsoon season was clearly seen in the both mean SSM and SWI climatology. Minimum difference between climatology and analysis was also found during the monsoon peak (Figure 8d). Analysed soil moisture at the surface level showed a somewhat weaker seasonal cycle (Figure 8a) whereas the analysed profile soil moisture was quite flat in 2009 (Figure 8b). There was a noticeable jump in the soil moisture analysis, following PS23 model upgrade and comparably weak seasonal trend following ASCAT assimilation in PS24 changes. The offset between climatology and analysis was large for the top 1 metre layer, ranging between 15% and 25%. Given the theoretical background of the scatterometer retrieval, it is not surprising that the correlations between climatology and analysis also exhibited a strong seasonal cycle (Figure 8c), with observed maximum correlation in August and September 2010 ($r = 0.83$; $p < 0.001$) and minimum correlation in December 2009 and January 2010 ($r = 0.46$) for the surface soil moisture. Given the very similar design of ERS and ASCAT scatterometers, a positive impact of ASCAT surface soil wetness assimilation was generally expected. Correlation between the climatology and analyses for the top 1m layer, on the other hand, showed a tighter seasonal correlation in 2010 compared to 2009.

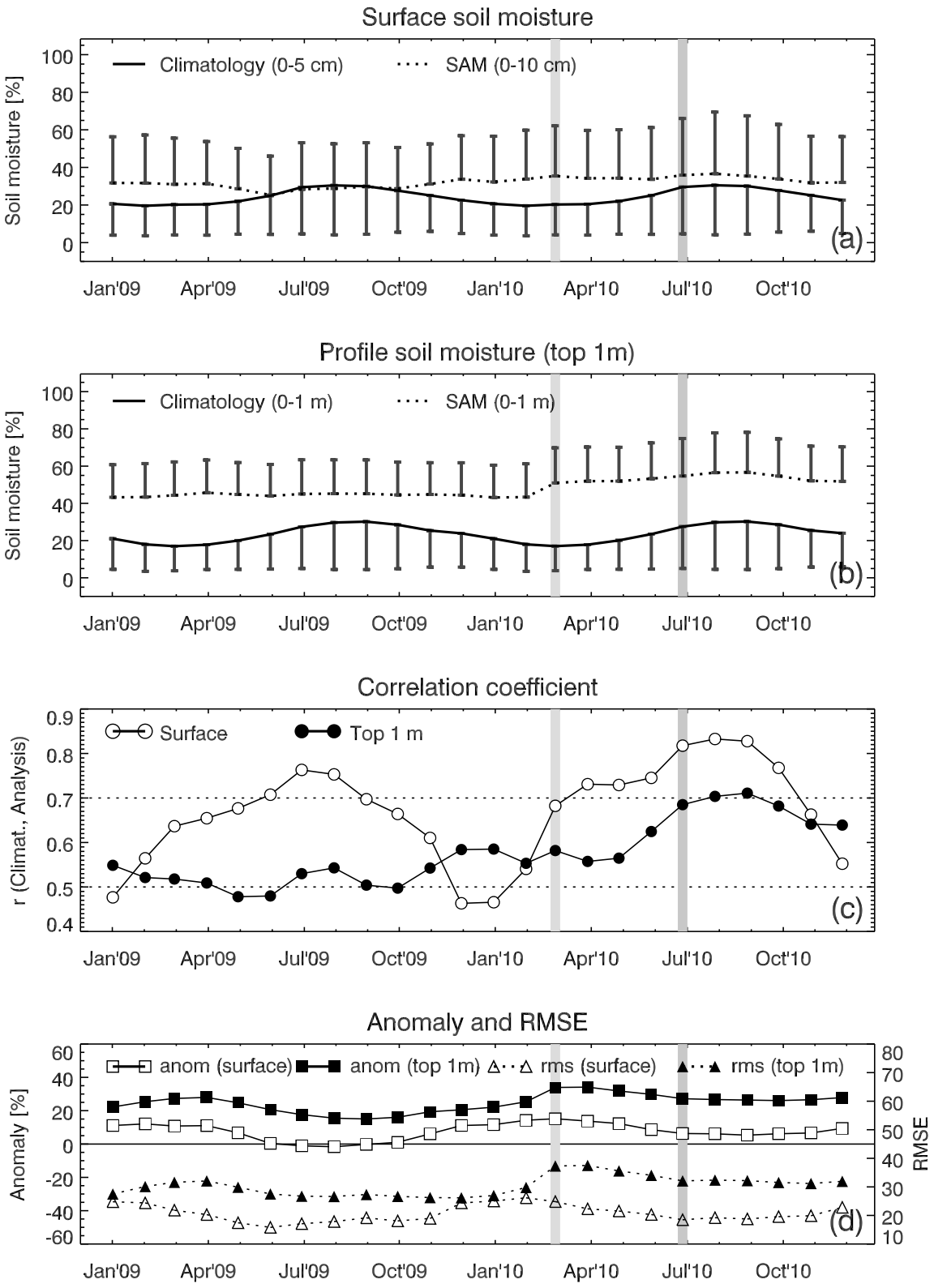

Figure 8: Time-evolution of monthly ESCAT climatology and UM soil moisture analyses showing domain average (standard deviations as vertical bars, shown on one side of the average line for clarity) monthly soil moisture at surface layer (a) and for 1m layer (b), monthly correlation between climatology and analysis (c), and monthly anomaly (departure from climatology) and RMSE (d).

3.2.4 Soil moisture anomaly

In this section we show departures of soil moisture content analysis from the climatology in 2009 and 2010 for the surface (Figure 9) and top 1m layer (Figure 10). The main purpose of this exercise was to identify regions where the analyses were consistently different from the climatology, which may further explain the uncertainties associated with either the scatterometer retrieval or the model analysis. The mean anomalies for all months, except Jul-Aug-Sep 2009 (Table 4), were positive meaning the analyses were wetter than the norm. It is worth to mention that the climatology surface moisture represents information on the top 5cm only which was compared with the model soil moisture for the top 10 cm. The deep soil moisture content is expected to be higher than the topsoil after the precipitation events during the monsoon season. Persistent negative surface soil moisture anomalies were observed over the Himalayan mountain region during the winter months and over the Arabian Peninsula during summer monsoon period. Positive surface soil moisture anomalies were observed over the Ethiopian highlands. It is known that the ESCAT $\sigma^0_{wet}(40)$ does not capture the saturated conditions in some arid regions. Although a bias correction has been applied to $\sigma^0_{wet}(40)$, the anomaly observed in the Arabian Peninsula was thought to have links to the uncertainties associated with ESCAT reference backscatter for saturation condition.

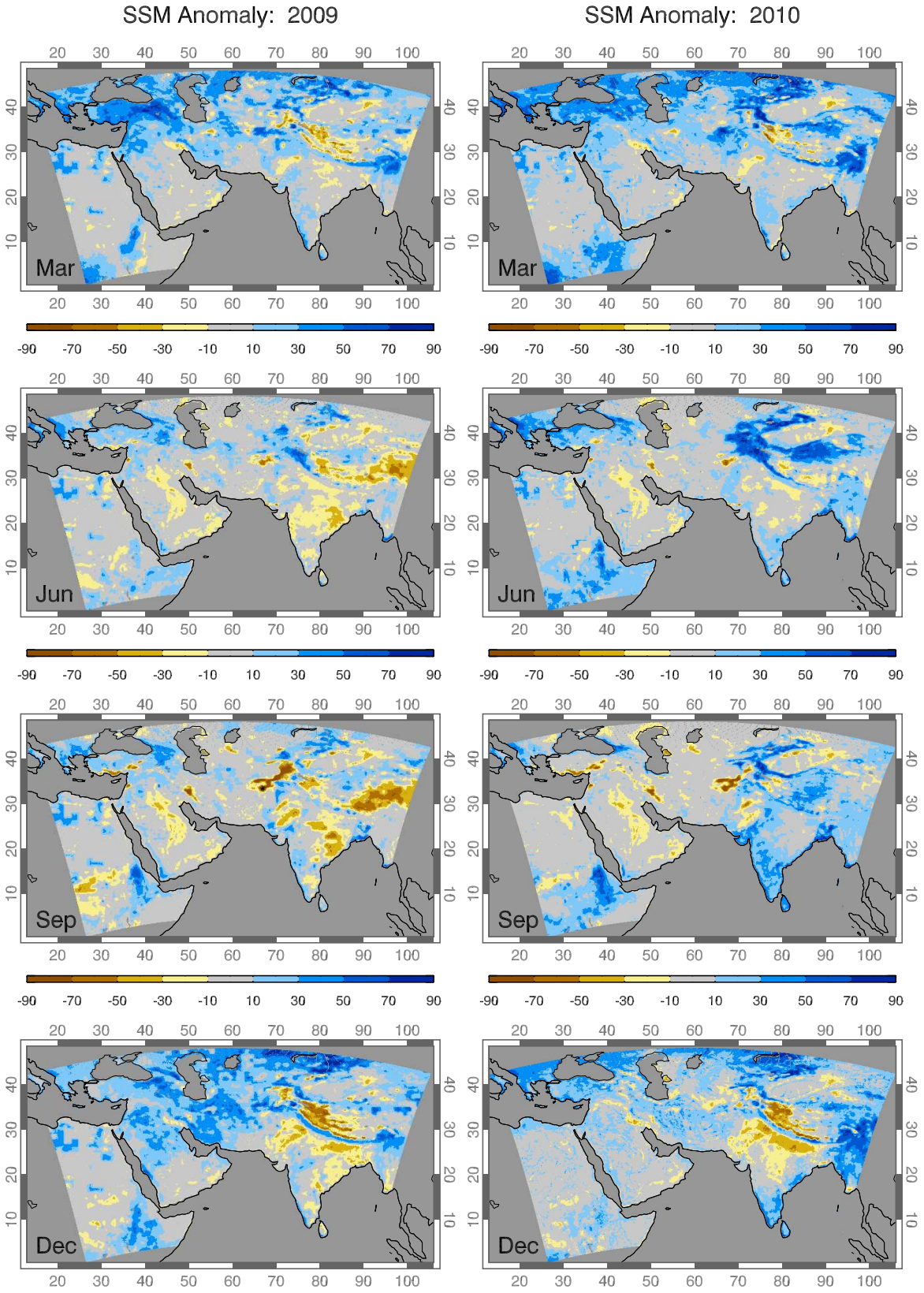

Figure 9: Departure of Model soil moisture (0-10cm) from climatology (0-5cm). The blue and brown shades indicate wet and dry regions w.r.t. climatology, respectively; grey shades indicate regions agreeing within 10% of climatological norm.

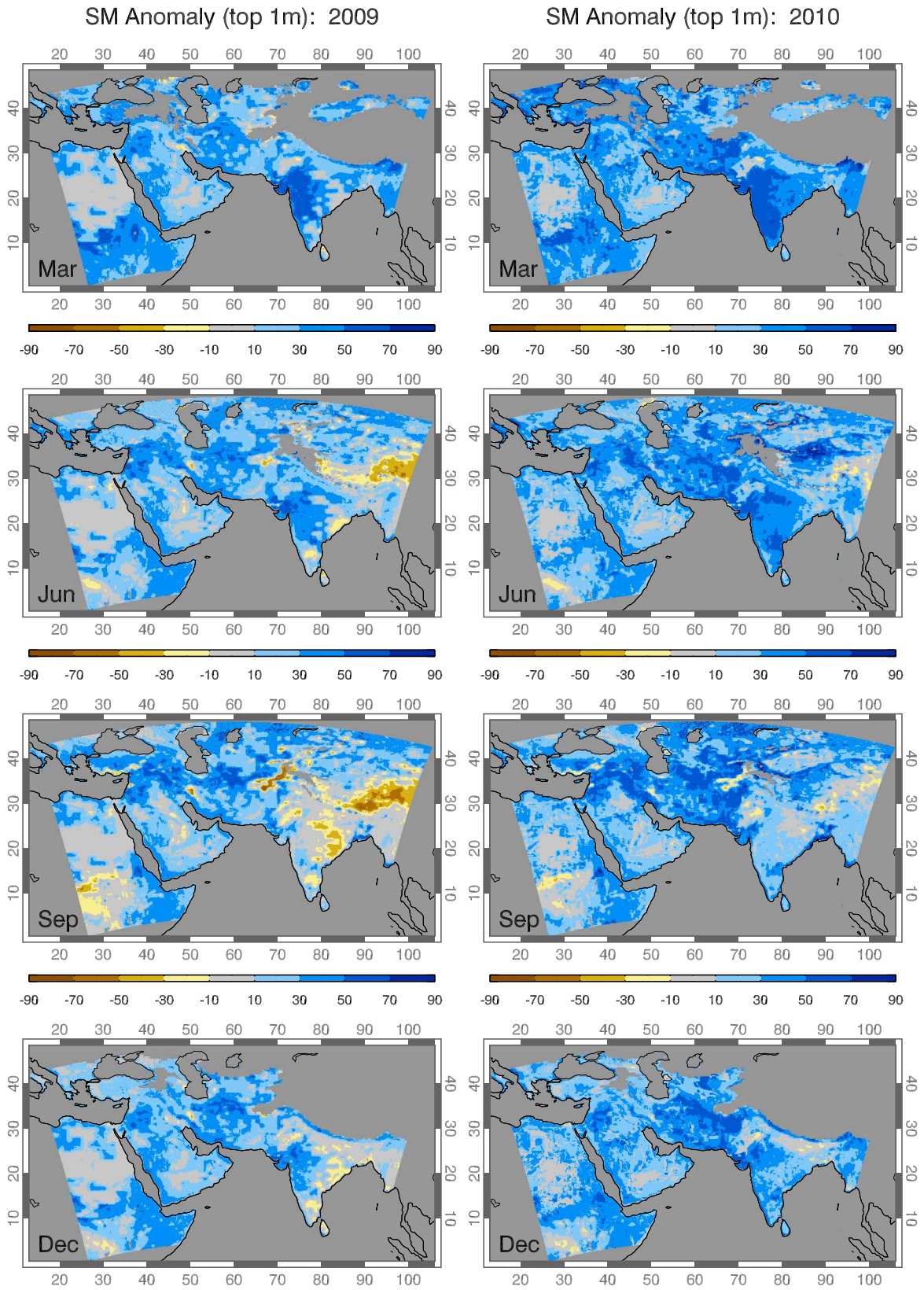

Figure 10: Same as Figure 9 but for the top 1m layer.

Table 4: Monthly correlation coefficients (r between climatology and model analyses) and anomaly (analysis - climatology) metrics: average (mean), median (med), standard deviation (stdev) and skewness (skew) for surface and top 1 m layers.

Month'	Surface layer					Top 1 metre				
Year	r	mean	med	stdev	skew	r	mean	med	stdev	skew
Jan'09	0.48	11.20	8.22	22.28	0.17	0.55	22.23	22.94	16.18	-0.16
Jan'10	0.46	11.74	8.42	22.36	0.24	0.59	22.12	22.71	15.43	-0.12
Feb'09	0.56	12.21	8.42	21.36	0.27	0.52	25.39	26.63	16.20	-0.13
Feb'10	0.54	14.45	10.8	22.25	0.22	0.55	25.36	26.72	15.63	-0.13
Mar'09	0.64	10.85	7.02	18.99	0.33	0.52	27.34	28.65	15.83	-0.16
Mar'10	0.68	15.18	11.34	19.66	0.46	0.58	33.93	34.28	15.51	-0.17
Apr'09	0.66	11.06	9.06	17.06	0.13	0.51	27.97	28.97	15.72	-0.14
Apr'10	0.73	13.78	10.55	17.54	0.67	0.56	34.13	34.51	15.52	-0.15
May'09	0.68	6.72	4.93	16.08	0.19	0.48	24.75	25.74	16.71	-0.35
May'10	0.73	12.27	8.76	17.70	0.68	0.56	31.84	32.38	15.90	-0.12
Jun'09	0.71	0.36	0.19	15.81	-0.01	0.48	20.61	22.21	18.24	-0.75
Jun'10	0.75	08.62	4.70	18.39	0.94	0.62	29.79	30.76	16.47	-0.17
Jul'09	0.76	-1.08	-0.78	17.07	-0.22	0.53	17.64	19.30	20.09	-0.78
Jul'10	0.82	6.31	3.91	17.37	0.55	0.69	27.20	27.84	17.05	-0.13
Aug'09	0.75	-1.65	-0.52	17.78	-0.51	0.54	15.53	16.92	21.63	-0.56
Aug'10	0.83	6.13	3.38	18.19	0.49	0.70	26.70	27.05	18.30	-0.07
Sep'09	0.70	-0.27	0.66	19.15	-0.74	0.50	15.02	16.87	22.82	-0.67
Sep'10	0.83	5.33	2.74	18.00	0.20	0.71	26.40	26.65	18.39	-0.10
Oct'09	0.66	1.04	0.75	18.05	-0.27	0.50	16.06	18.16	21.31	-0.72
Oct'10	0.77	6.08	3.58	18.57	0.18	0.68	26.12	26.56	17.67	-0.09
Nov'09	0.61	6.07	4.96	17.96	-0.24	0.54	19.38	20.92	17.71	-0.39
Nov'10	0.66	6.64	5.11	18.75	-0.03	0.65	26.69	27.74	16.10	0.14
Dec'09	0.46	11.16	9.62	21.76	-0.16	0.58	20.56	21.03	16.19	-0.14
Dec'10	0.55	9.40	7.57	20.79	0.01	0.64	27.87	29.00	15.58	-0.15

Backscatter from mountainous regions can be prone to several distortions, such as calibration errors due to deviation of the surface from the assumed ellipsoid, influence of permanent snow and ice cover, reduced sensitivity due to highly variable surface conditions like rock and forest cover, etc. Scatter between SAM orography and surface soil moisture anomaly for January 2009, for an example, clearly showed two clusters separated at around 2km (Figure 11). Positive and negative trends of the surface soil moisture in the highlands corresponded to the anomalies observed in the Ethiopian highland and the Himalayan mountain range. The ESCAT climatology dataset has additional quality flag indicators for SNOW (probability and fraction of snow cover), FROZEN (probability

of soil temperature below 0°C), WATER (open water surfaces such as lakes, rivers, wetlands, etc.) and TOPO (topographic complexity) which was derived from GTOPO30 data as the standard deviation of elevation normalised to values between 0 and 100. Although we have excluded the available flags in the current study, it clearly highlighted the importance of use of quality flags *vis-à-vis* ESCAT soil moisture climatology products in future studies.

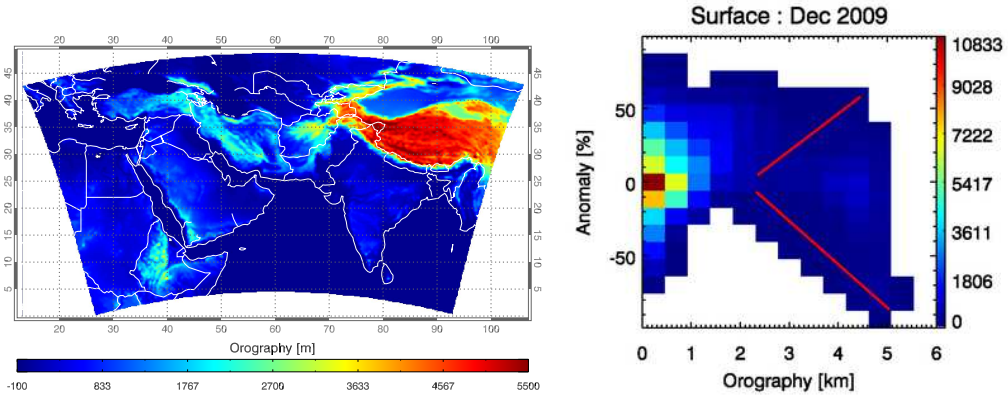

Figure 11: SAM orography (left) and density plot of surface soil moisture anomaly versus orography (right).

4 Outlook

A monthly soil moisture climatology dataset based on ~13 year time series of ESCAT surface soil moisture (top 5cm) and soil water index (top 1m) records was generated and the dataset was compared against the Met Office soil moisture analysis over a period of 2009 and 2010 in the Southern Asia Crisis Area Model domain. The comparison highlighted several improvements in the model analyses following the UM upgrade and ASCAT soil wetness assimilation, as well as the uncertainties associated with the climatology in certain regions within the SAM domain:

- Realistic surface and profile soil moisture following improved model resolution and hydrology (in PS23);
- Better representation of *Talkimakan* desert in both ancillary and soil moisture analysis following the implementation of Harmonized World Soil Database (HWSD) soil in PS23;
- Analysed soil moisture explained more than 50% of climatology surface soil moisture variance in 3 out of 12 months in 2009 compared to 7 out of 11 months in 2010, indicating the benefits of UM model upgrade (in PS 23) and assimilation of ASCAT surface soil wetness (in PS24);
- It was evident that the surface soil moisture climatology may be associated with uncertainties arising from topographic complexity which was apparent in winter months; therefore, it is recommended to use the quality flags provided with the climatology dataset.

- Surface soil moisture climatology may have wet bias in some arid regions over the Arabian Peninsula as a result of the bias in the reference backscatter at saturation.

In general, the year 2009 was observed to be relatively drier than 2010 in SAM and especially over the Indian subcontinent, which was also evident from the National Centre for Environment Prediction (NCEP) precipitation anomaly dataset[5]. The 2010 Pakistan floods which started in July 2010 following heavy monsoon rains in the proximity of the Indus River basin was also noticed clearly in SAM surface soil moisture anomalies in August 2010 (Annex-2). This preliminary study encourages a comprehensive global comparison of ESCAT climatology with Met Office global soil moisture analysis and climatology. However, a global comparison will require the tropical forests properly flagged (currently not available in ESCAT climatology, but a monthly vegetation atlas may be used in future).

Within the scatterometer family, the instruments on ERS-1 and ERS- 2 and ASCAT have been used to retrieve global soil moisture content in a consistent manner. Although NASA's quick scatterometer (QuikSCAT, operating in Ku-band) has potential to capture the temporal soil moisture variation at large scale, it was found to be less reliable showing a poor visual coherence due to the high observational frequency, existence of noise and overpass time difference [14]. In the radiometer family, the Advanced Microwave Scanning Radiometer (AMSR-E on Aqua) makes global observation of soil moisture; however, the C-band observations were reportedly contaminated with anthropogenic Radio Frequency Interference (RFI) in some areas [3]. The AMSR-E soil moisture data showed a significant lack of seasonal soil moisture dynamics [18]. ESA's Soil Moisture and Ocean Salinity (SMOS) mission has completed a year in orbit making global observations of soil moisture over Earth's landmasses. With higher sensitivity to soil moisture due to L-band measurements, SMOS is expected to provide improved accuracy in observing soil moisture variability and retrieval of volumetric soil moisture content. We propose to use the SMOS data for verification (and possibly assimilation, if available in near-real-time) of model analysis in near future.

Acknowledgements The authors wish to express their gratitude to Wolfgang Wagner for providing access to Level 2 ESCAT soil moisture data, and John Eyre, Imtiaz Dharssi and Ric Crocker for their helpful comments and assistance.

[5] Jun 2009 http://bit.ly/hUFCNq; Jun 2010 http://bit.ly/hoxdRh
Jul 2009 http://bit.ly/fprjs9; Jul 2010 http://bit.ly/fJUiY7
Aug 2009 http://bit.ly/dKPj4y; Aug 2010 http://bit.ly/dXtgu3
Sep 2009 http://bit.ly/fzfQ0q; Sep 2010 http://bit.ly/fJCOtr

5 Annex-1

5.1 Normalisation of σ^0

Because the intensity of backscatter signal strongly depends on the incidence angle (θ), it can not be used directly for an unambiguous soil moisture retrieval. Therefore, the measurements need to be normalised to a reference incidence angle (40°), which is performed by using a second order polynomial of the form:

$$\sigma^0(40,t) = \sigma^0(\theta,t) - \sigma'(40,t)(\theta - 40) - \frac{1}{2}\sigma''(40,t)(\theta - 20)^2 \tag{5}$$

where σ' and σ'' are respectively the first and second derivatives of σ^0 with respect to θ. The reference angle is set to 40° in order to minimize extrapolation errors [23]. The parameters of this model, the slope σ' and the curvature σ'', are determined from simultaneous multi-incidence angle observations:

$$\sigma'\left(\frac{\theta_{mid} - \theta_{fore/aft}}{2}\right) = \frac{\sigma^0_{mid}\left(\theta_{mid}\right) - \sigma^0_{fore/aft}\left(\theta_{fore/aft}\right)}{\theta_{mid} - \theta_{fore/aft}} \tag{6}$$

Having a large set of samples evenly distributed over the entire incidence angle range, $\sigma'(40)$ and $\sigma''(40)$ can be derived by fitting a linear model of the form:

$$\sigma'(\theta) = \sigma'(40) + \sigma''(40)(\theta - 40) \tag{7}$$

The exact shape of the polynomial expressed in equation 5.1 depends on the land surface properties, such as the state of vegetation and the roughness of the surface. Less rough surfaces with little vegetation result in a steep decline of σ^0 with respect to θ and therefore low, negative $\sigma'(40)$ values. Increased vegetation and rough surfaces generally result in higher $\sigma'(40)$ values. Each of the slope and the curvature thus show a distinct annual cycle, determined by vegetation growth and decay.

6 Annex-2

6.1 Pakistan flooding (2010)

Heavy rainfalls of more than 200 millimetres recorded during the four day wet spell of July 27 to July 30, 2010 in the provinces of Khyber Pakhtunkhwa, and Punjab[6] which led to the disastrous flooding in the Indus basin. Directly affecting around 20 million people. Figure 12 highlights the correspondence between the surface area affected by heavy precipitation in July 2010 and the SAM surface soil moisture anomaly in the following month.

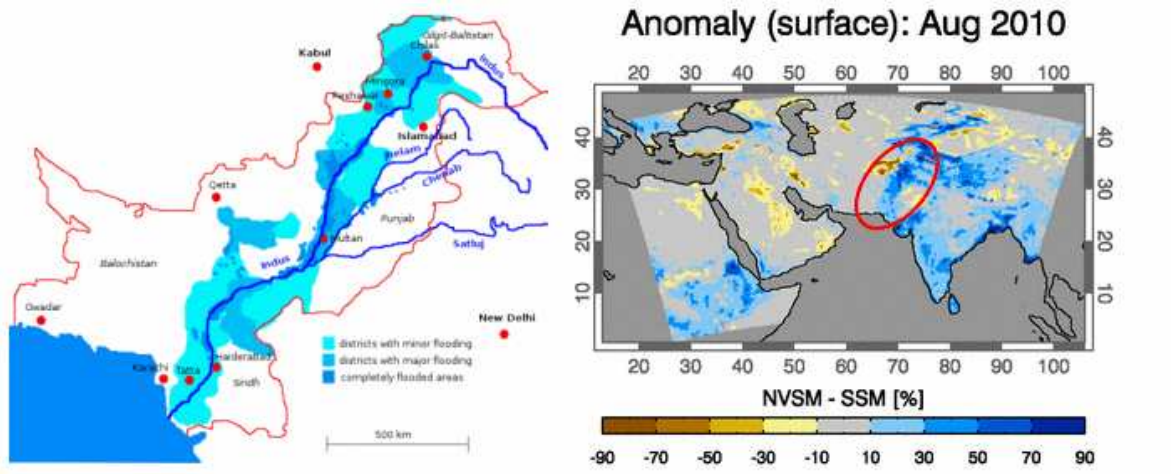

Figure 12: Areas affected by 2010 Pakistan flood as of August 26 (left panel). The flood affected area map was adapted from Wikipedia under the Creative Commons license. SAM soil moisture anomaly at top 10cm layer shows a clear correspondence with the Pakistan flood event (highlighted in the right panel).

[6] http://www.pakmet.com.pk/FFD/index_files/rainfalljuly10.htm

7 Annex-3

Monthly climatology maps of ESCAT surface soil moisture and soil water index are demonstrated here. The full dataset including other metrics and maps can be made available upon request.

7.1 Surface Soil Moisture monthly climatology

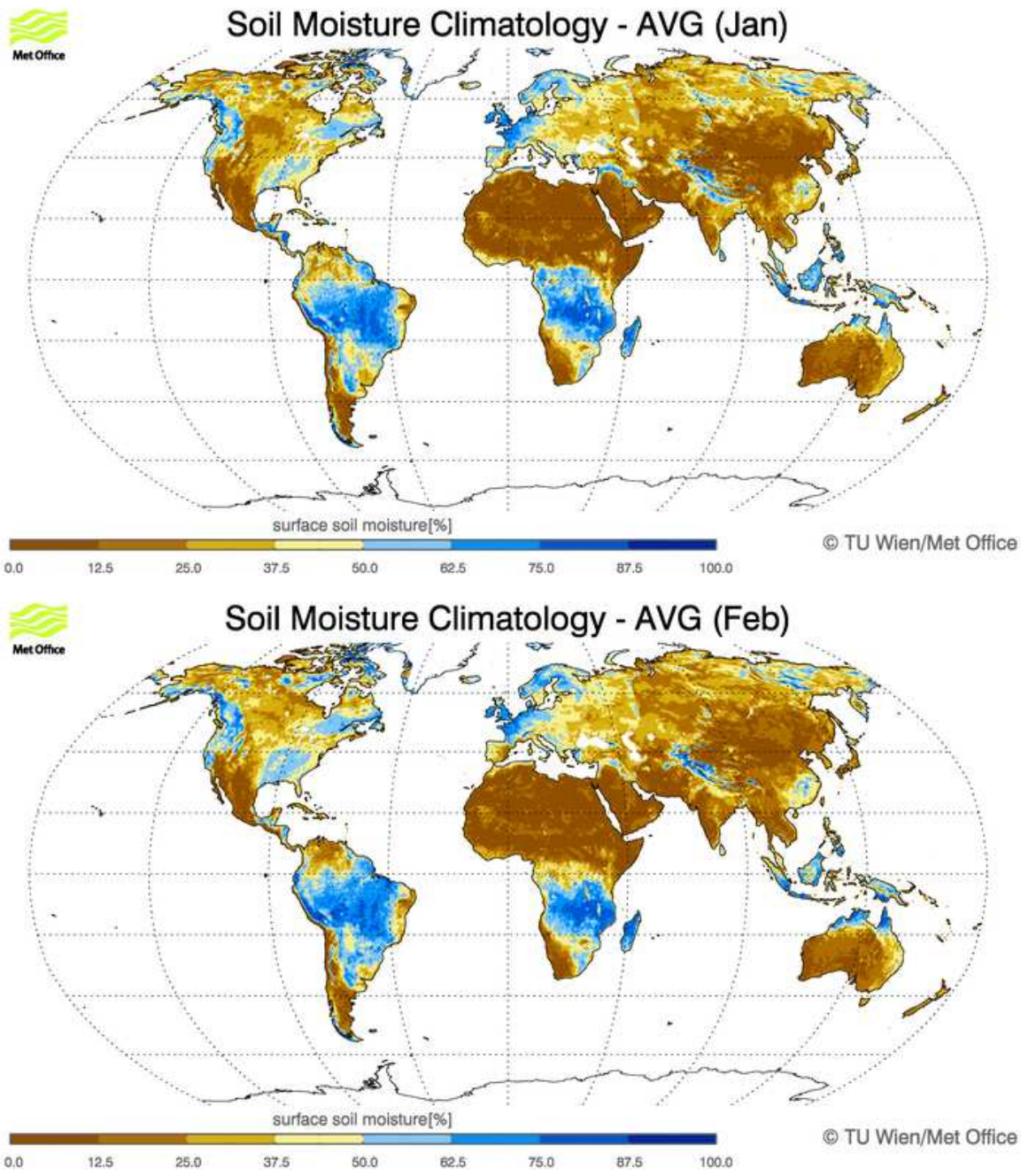

Figure 13: SSM climatology - January (top), February (bottom)

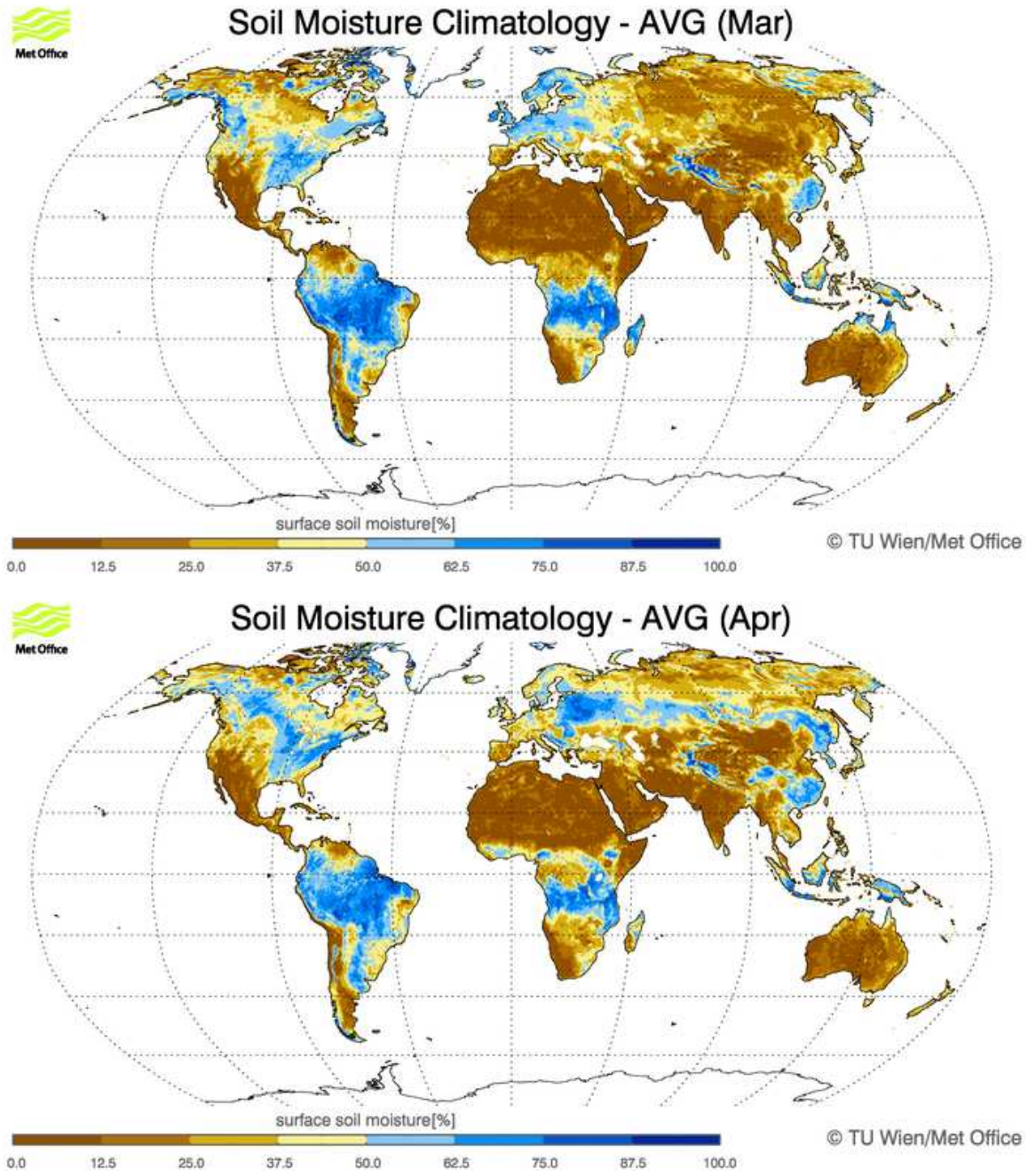

Figure 14: SSM climatology - March (top), April (bottom)

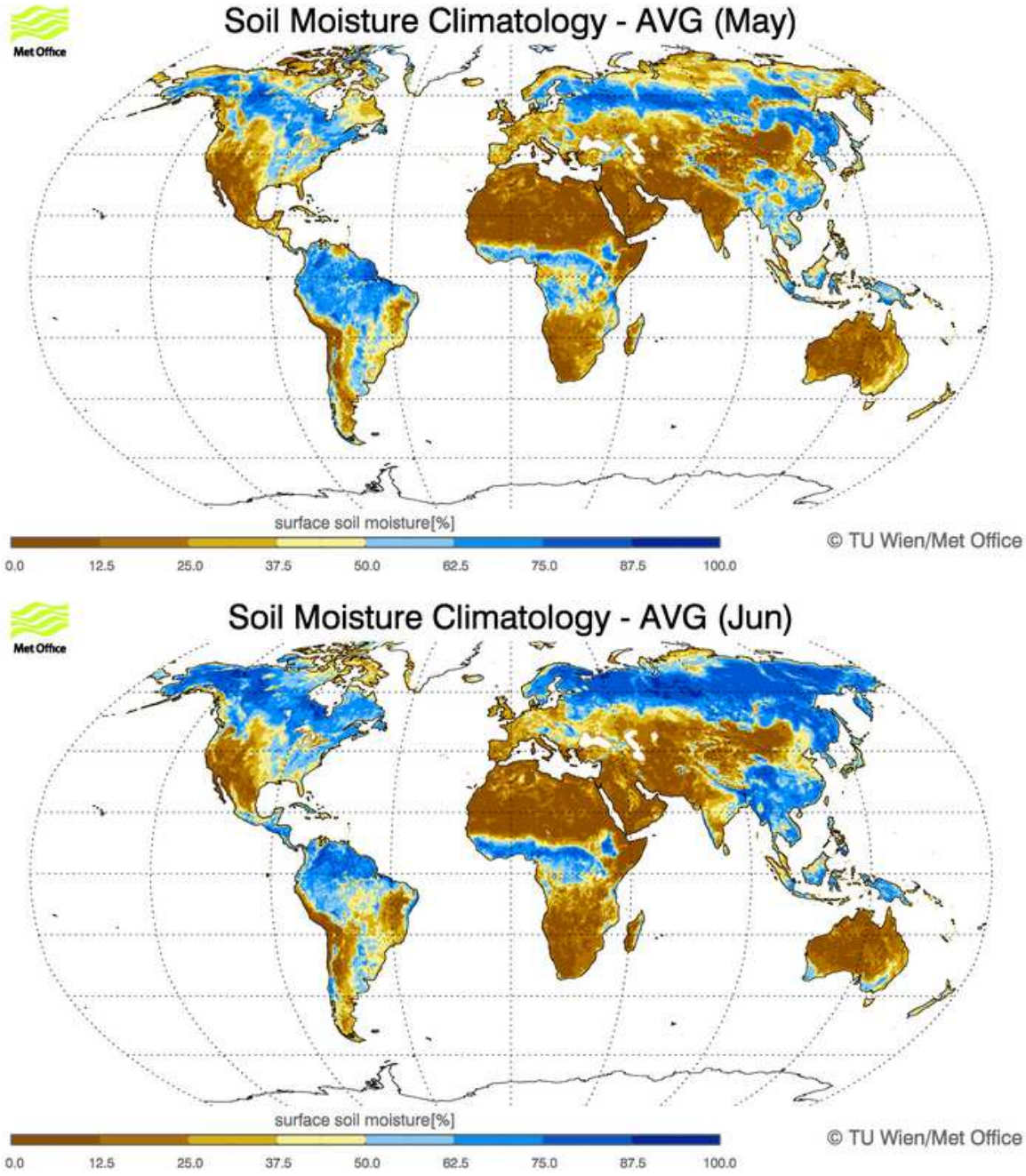

Figure 15: SSM climatology - May (top), June (bottom)

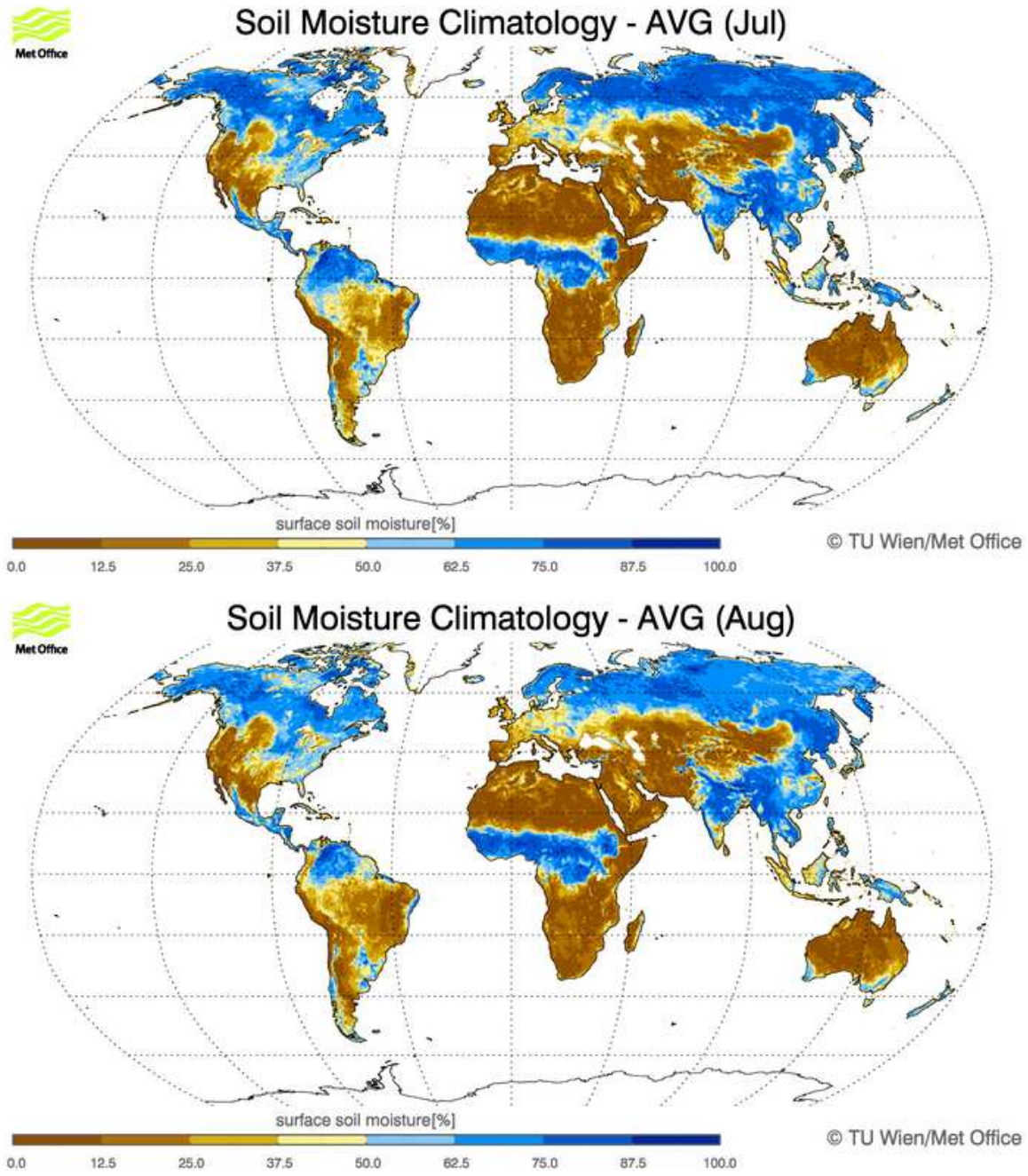

Figure 16: SSM climatology - July (top), August (bottom)

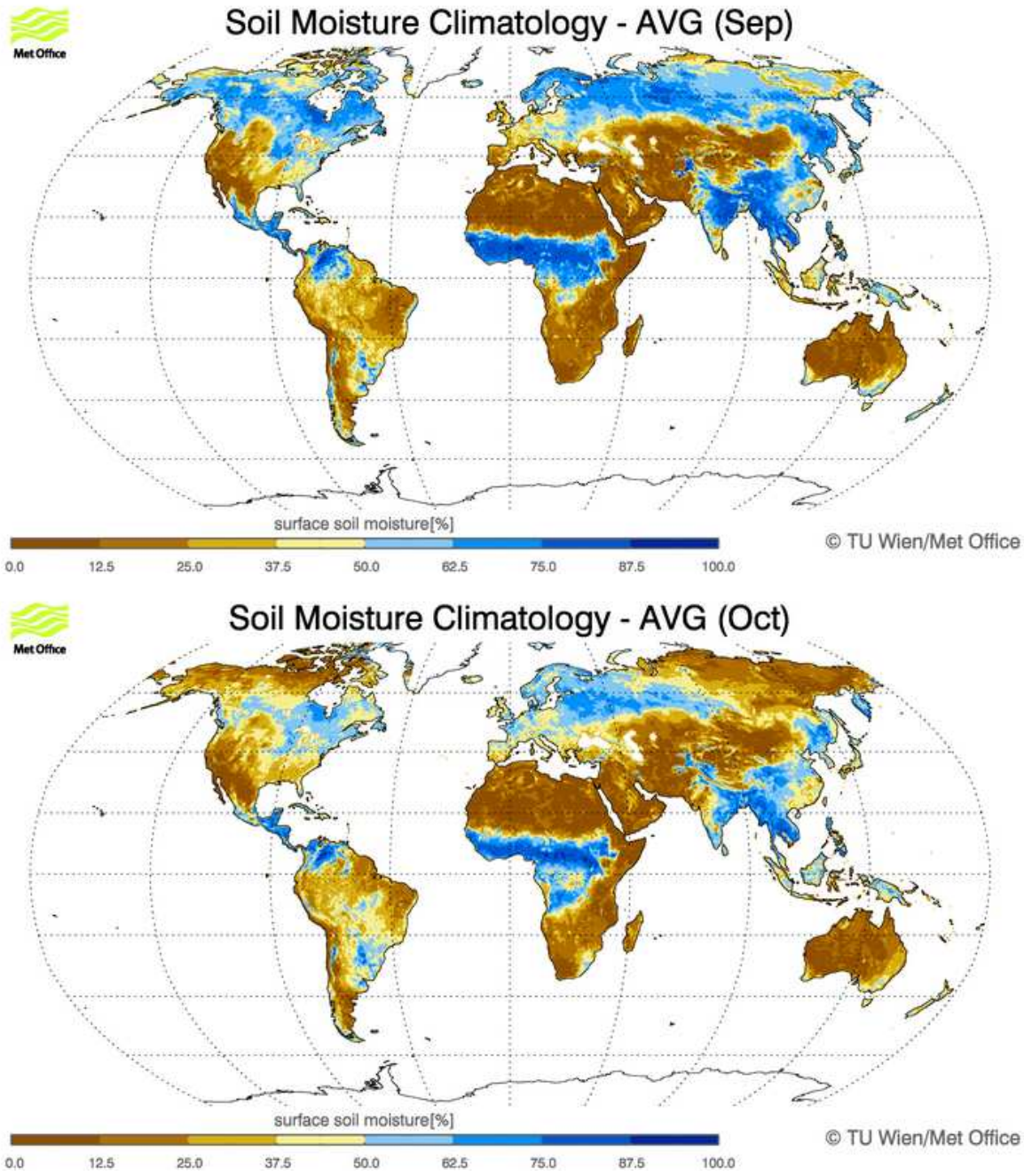

Figure 17: SSM climatology - September (top), October (bottom)

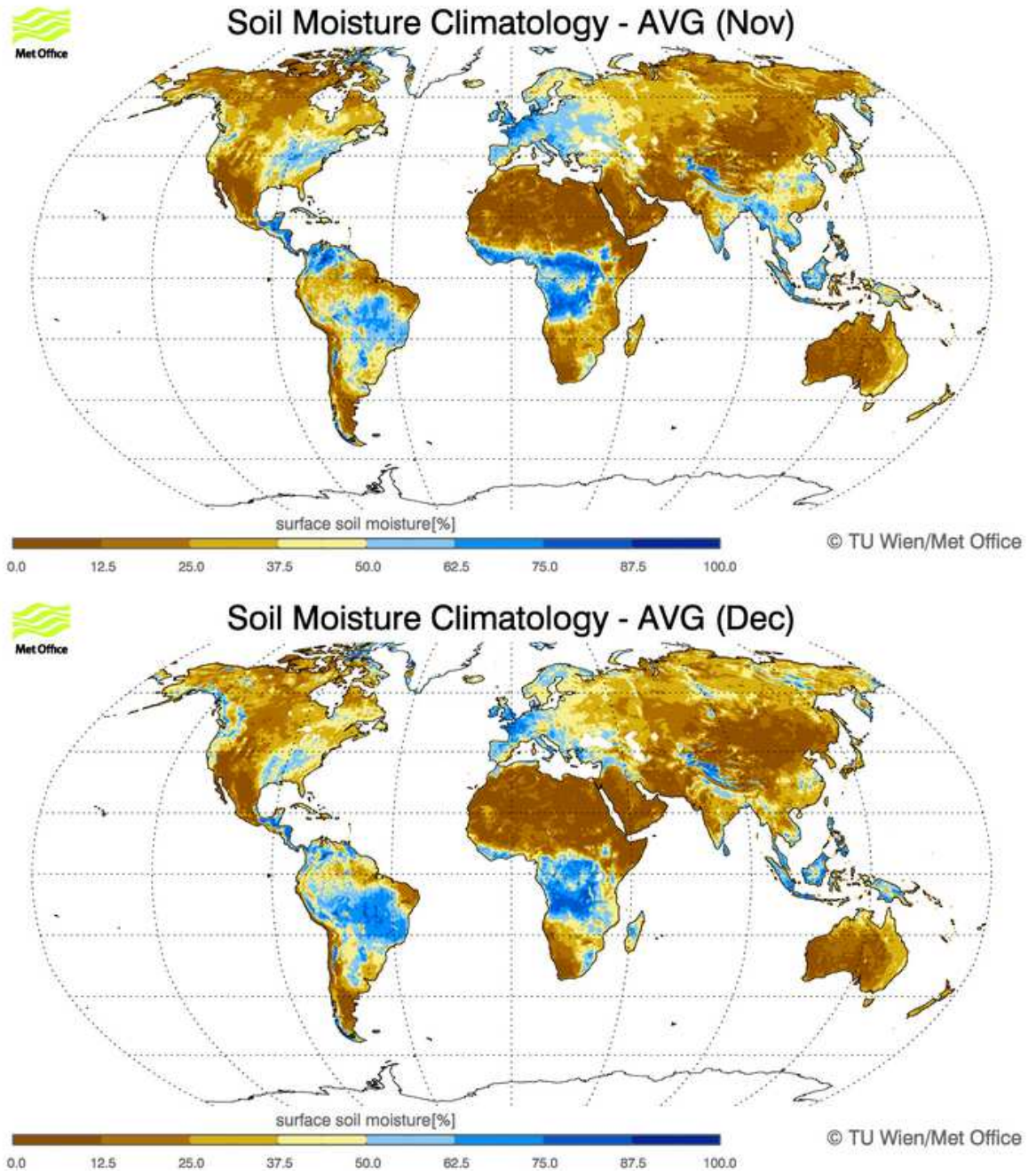

Figure 18: SSM climatology - November (top), December (bottom)

7.2 Soil Water Index monthly climatology

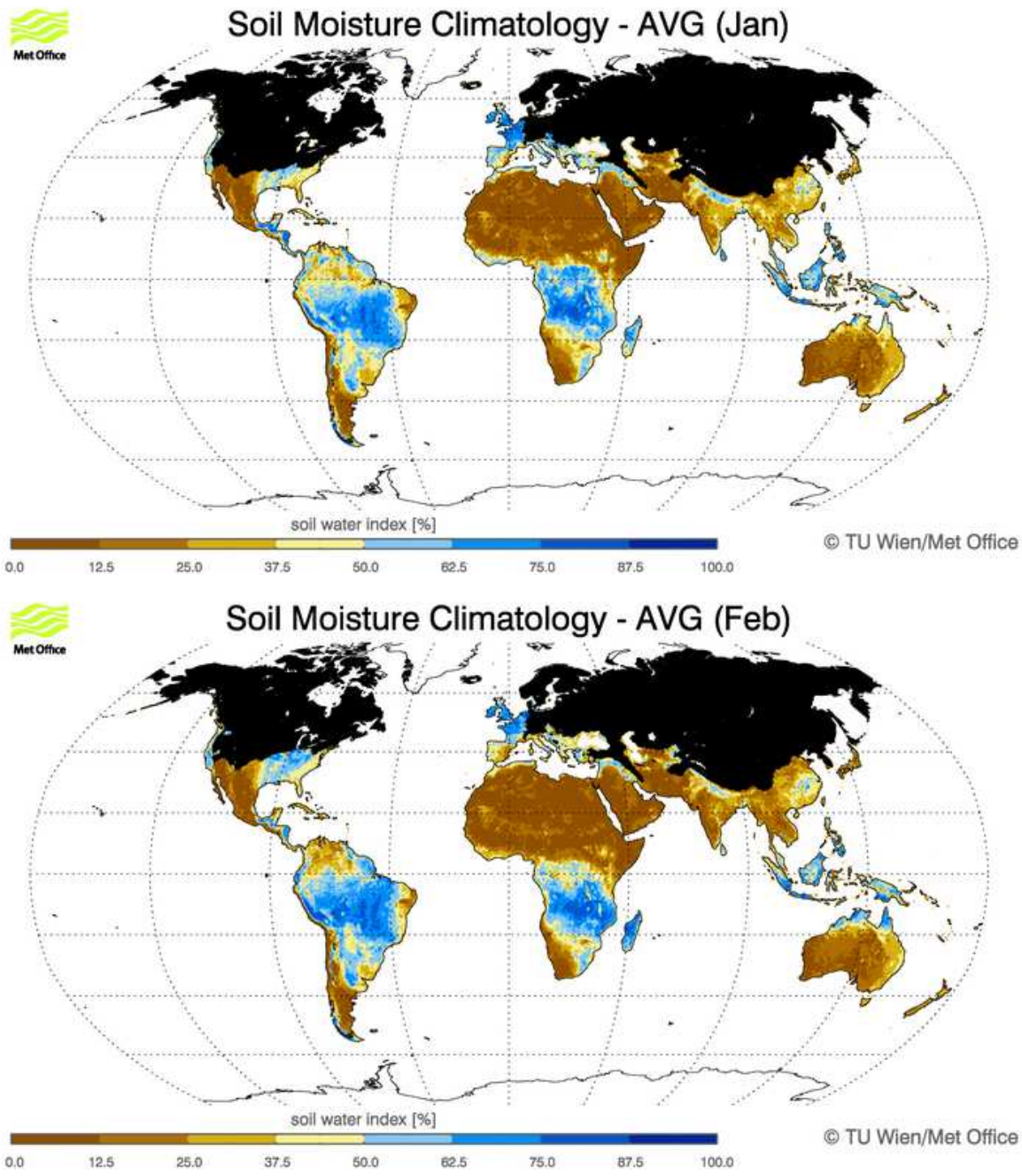

Figure 19: SWI climatology - January (top), February (bottom). Areas with no SWI retrievals (uncertainties due to snow and ice cover) are indicated with black colour.

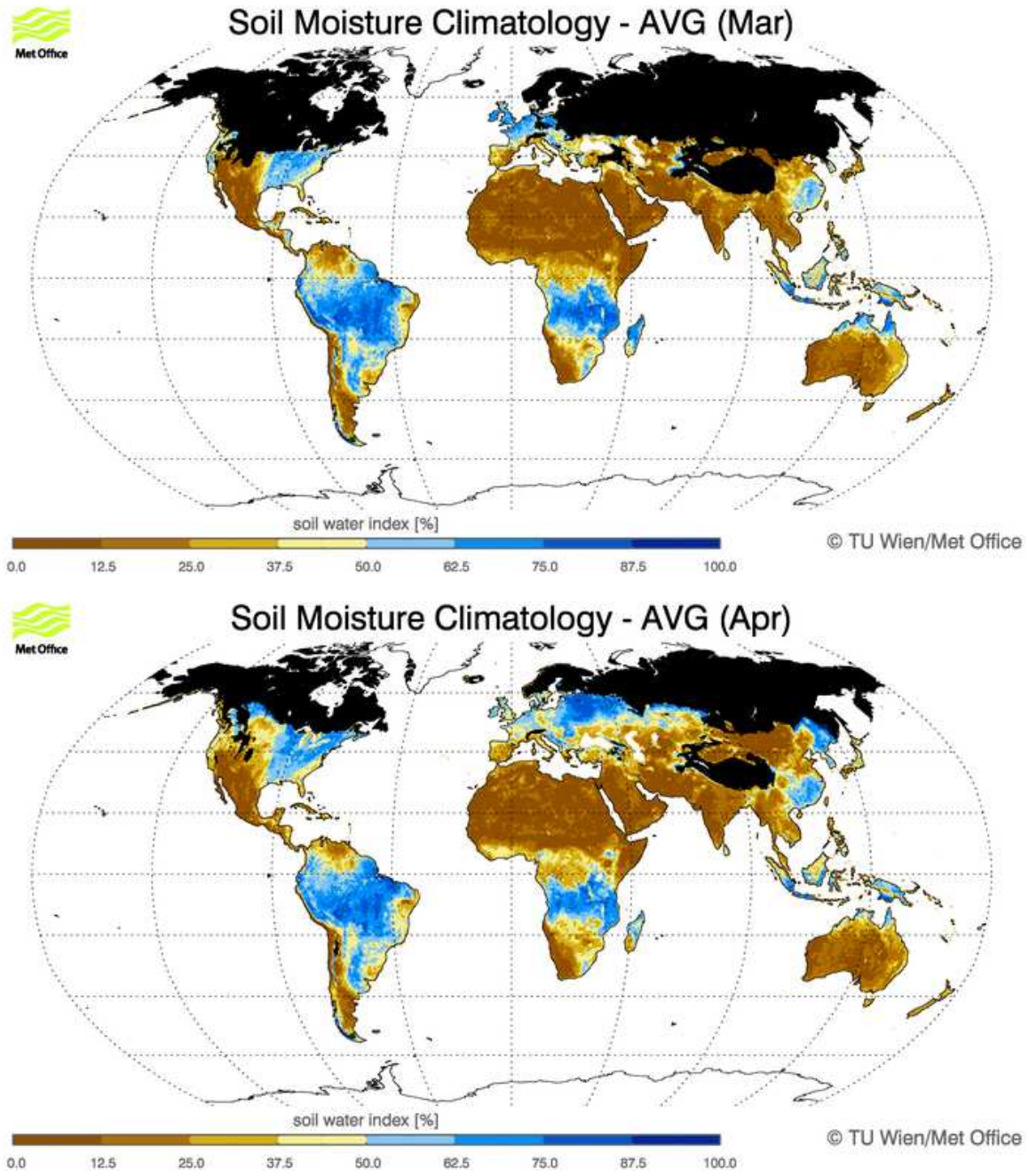

Figure 20: SWI climatology - March (top), April (bottom)

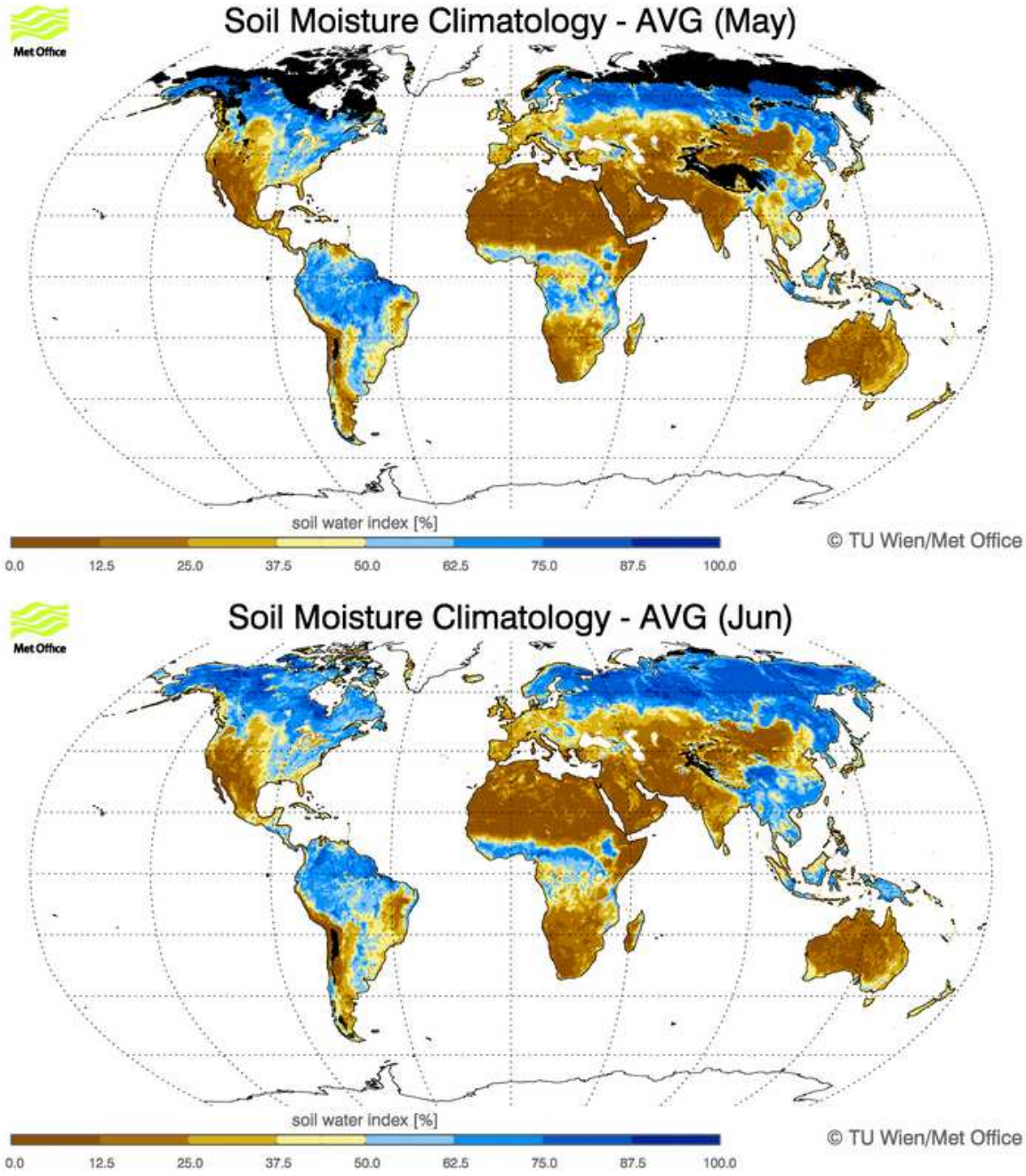

Figure 21: SWI climatology - May (top), June (bottom)

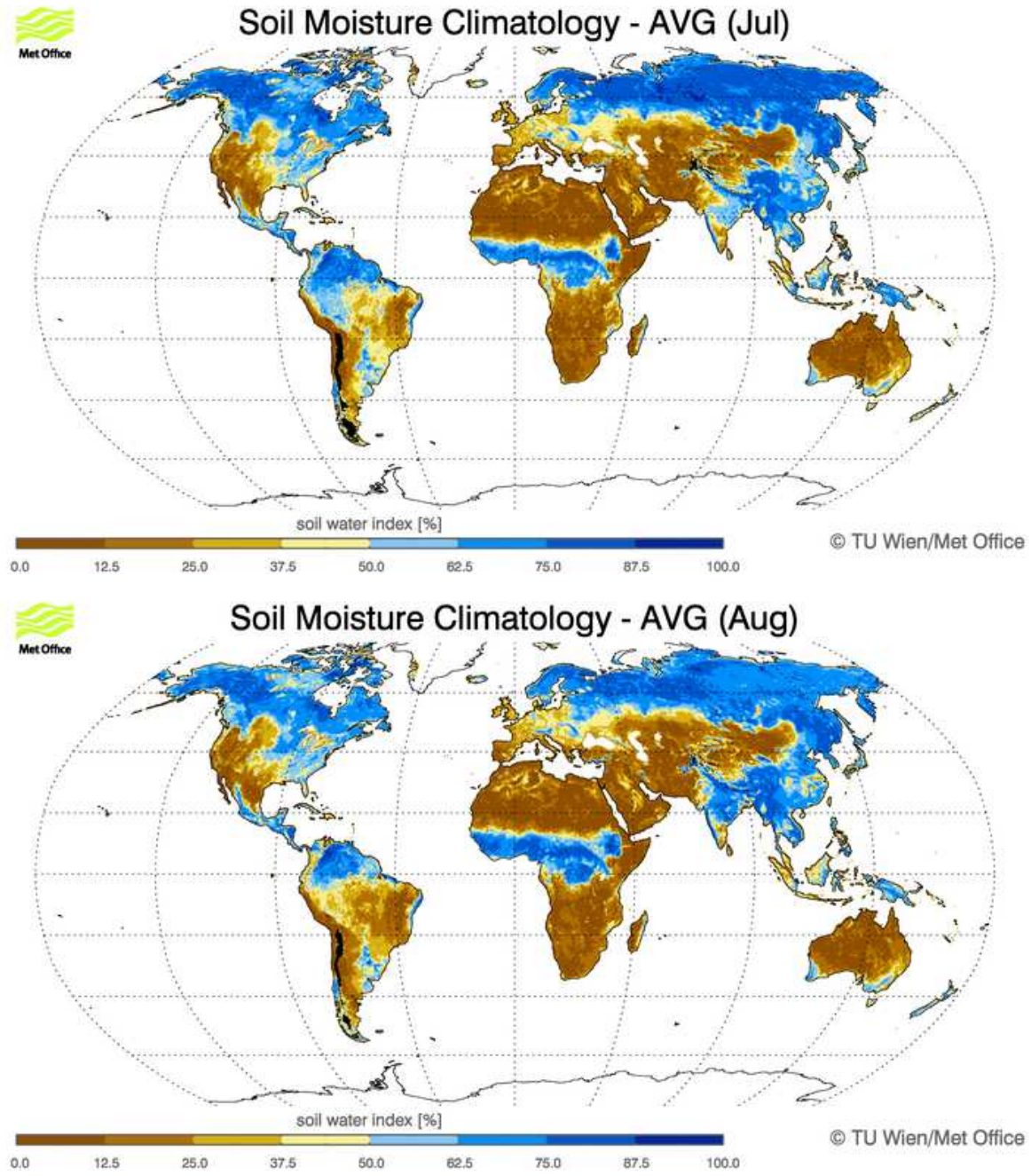

Figure 22: SWI climatology - July (top), August (bottom)

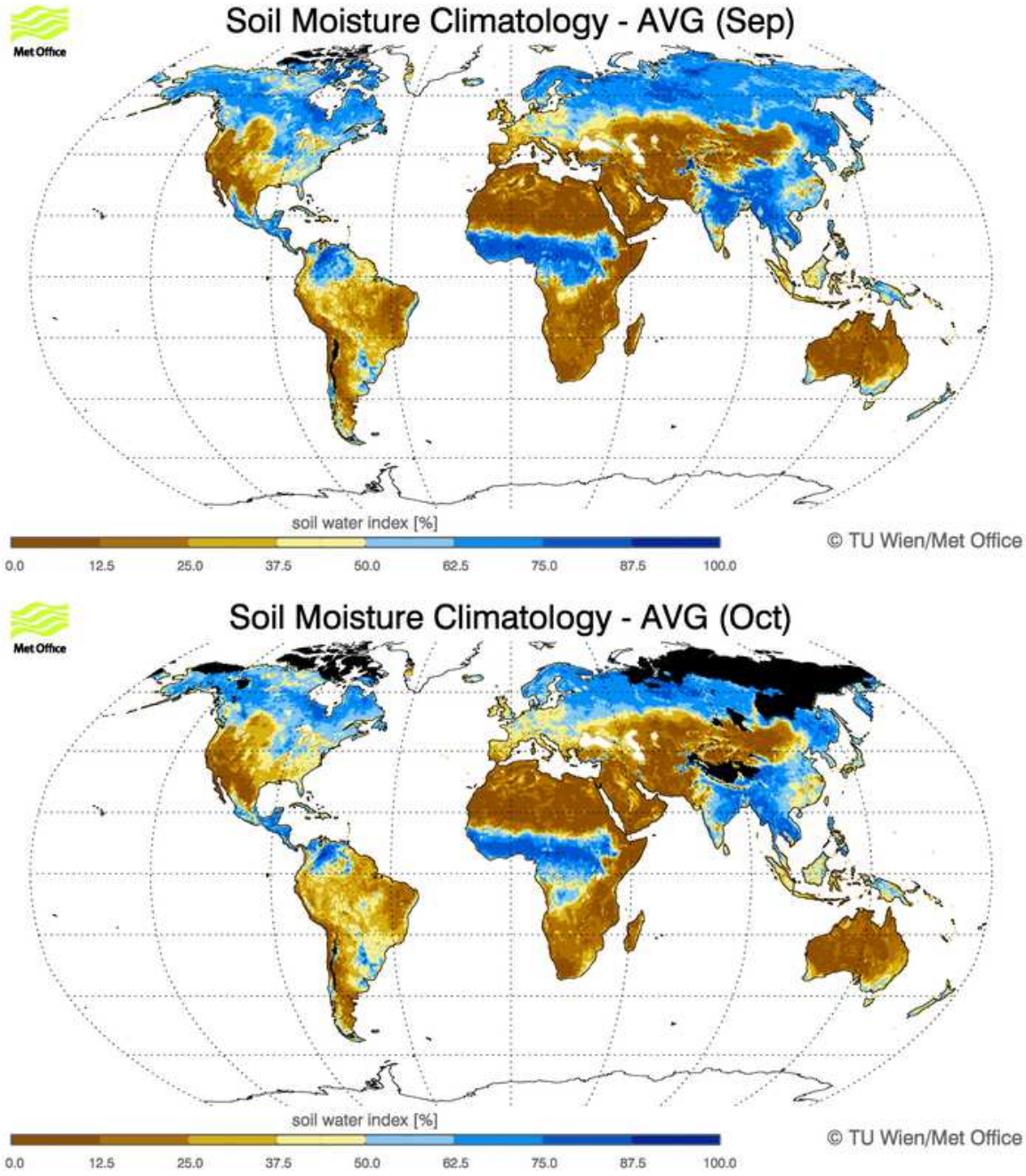

Figure 23: SWI climatology - September (top), October (bottom)

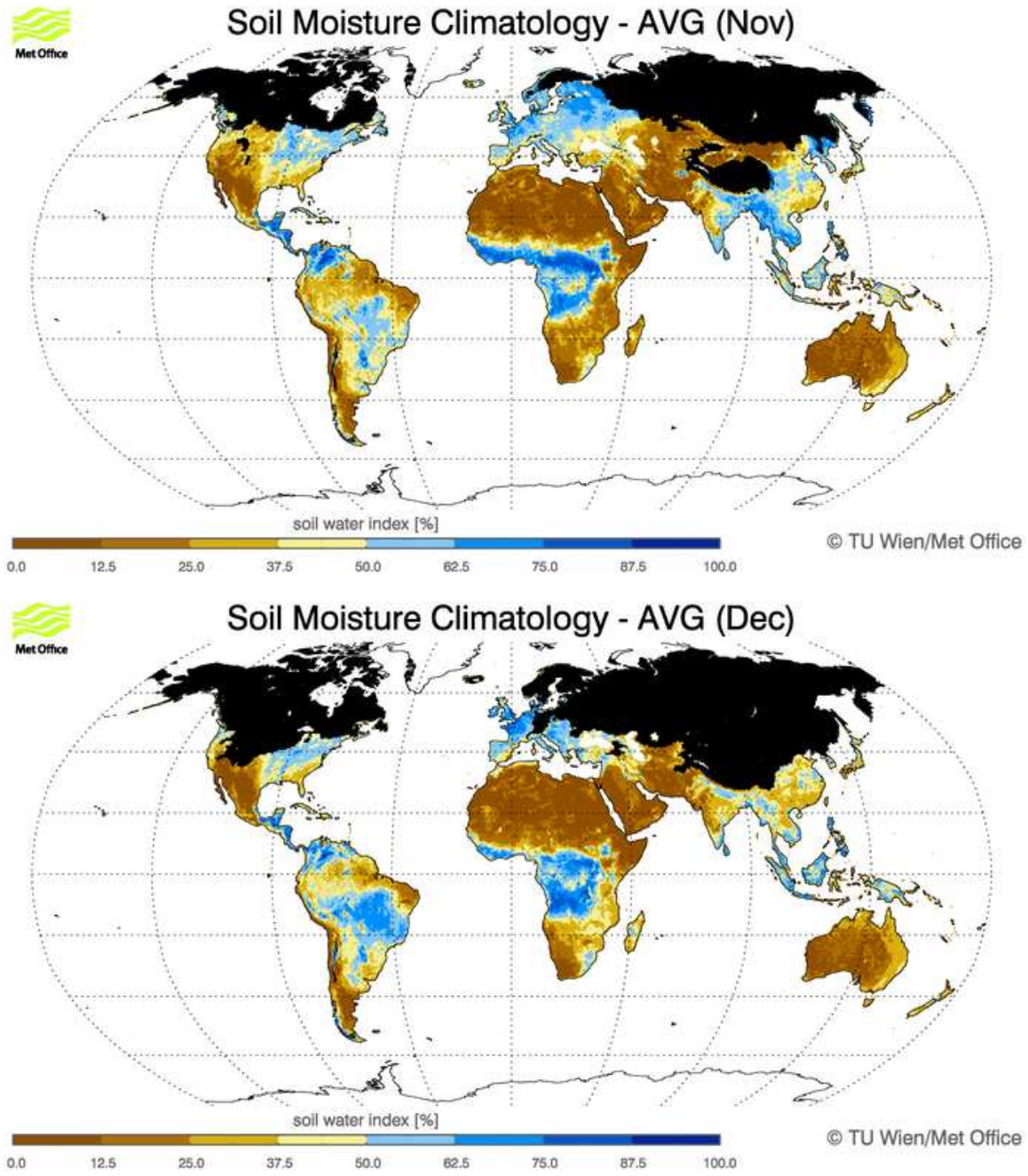

Figure 24: SWI climatology - November (top), December (bottom)

References

[1] A. Agusti-Panareda, G. Balsamo, and A. Beljaars. Impact of improved soil moisture on the ecmwf precipitation forecast in west africa. *Geophys. Res. Lett.*, 37(20):L20808, 2010.

[2] Z. Bartalis, V. Naeimi, S. Hasenauer, and W. Wagner. Ascat soil moisture product handbook. Technical Report 15, Institute of Photogrammetry and Remote Sensing, Vienna University of Technology, Nov 2008.

[3] R. Bindlish, T. J. Jackson, A. J. Gasiewski, M. Klein, and E. G. Njoku. Soil moisture mapping and amsr-e validation using the psr in smex02. *Remote Sensing of Environment*, 103(2):127–139, 2006. Bindlish, Rajat Jackson, Thomas J. Gasiewski, Albin J. Klein, Marian Njoku, Eni G.

[4] A. Ceballos, K. Scipal, W. Wagner, and J. Martinez-Fernandez. Validation of ers scatterometer-derived soil moisture data in the central part of the duero basin, spain. *Hydrological Processes*, 19(8):1549–1566, 2005.

[5] R. de Lange, R. Beck, N. van de Giesen, J. Friesen, A. de Wit, and W. Wagner. Scatterometer-derived soil moisture calibrated for soil texture with a one-dimensional water-flow model. *Ieee Transactions on Geoscience and Remote Sensing*, 46(12):4041–4049, 2008. de Lange, Reniko Beck, Rob van de Giesen, Nick Friesen, Jan de Wit, Allard Wagner, Wolfgang.

[6] I. Dharssi, K. Bovis, B. Macpherson, and C Jones. Assimilation of ascat surface soil moisture. Technical Report 545, Met Office, July 2010.

[7] P. A. Dirmeyer, Z. C. Guo, and X. Gao. Comparison, validation, and transferability of eight multiyear global soil wetness products. *Journal of Hydrometeorology*, 5(6):1011–1033, 2004.

[8] E. A. B. Eltahir. A soil moisture rainfall feedback mechanism 1. theory and observations. *Water Resources Research*, 34(4):765–776, 1998.

[9] R. Essery, M. Best, and P. Cox. Moses 2.2 technical documentation. Technical Report 30, Met Office, July 2001.

[10] B. Fontaine, S. Louvet, and P. Roucou. Fluctuations in annual cycles and inter-seasonal memory in west africa: rainfall, soil moisture and heat fluxes. *Theoretical and Applied Climatology*, 88(1-2):57–70, 2007. Fontaine, B. Louvet, S. Roucou, P.

[11] Daniel Hillel. *Introduction to Environmental Soil Physics*. Academic Press, 2003.

[12] Markus Kottek, Jurgen Grieser, Christoph Beck, Bruno Rudolf, and Franz Rubel. World map of the koppen-geiger climate classification updated. *Meteorologische Zeitschrift*, 15(3):259–265, 2006.

[13] B. Lehner and P. Doll. Development and validation of a global database of lakes, reservoirs and wetlands. *Journal of Hydrology*, 296(1-4):1–22, 2004.

[14] I. Mladenova, V. Lakshmi, J. P. Walker, D. G. Long, and R. De Jeu. An assessment of quikscat ku-band scatterometer data for soil moisture sensitivity. *Ieee Geoscience and Remote Sensing Letters*, 6(4):640–643, 2009. Mladenova, Iliana Lakshmi, Venkat Walker, Jeffrey P. Long, David G. De Jeu, Richard.

[15] V. Naeimi, Z. Bartalis, and W. Wagner. Ascat soil moisture: An assessment of the data quality and consistency with the ers scatterometer heritage. *Journal of Hydrometeorology*, 10(2):555–563, 2009. Naeimi, Vahid Bartalis, Zoltan Wagner, Wolfgang.

[16] V. Naeimi, K. Scipal, Z. Bartalis, S. Hasenauer, and W. Wagner. An improved soil moisture retrieval algorithm for ers and metop scatterometer observations. *Ieee Transactions on Geoscience and Remote Sensing*, 47(7):1999–2013, 2009. Naeimi, Vahid Scipal, Klaus Bartalis, Zoltan Hasenauer, Stefan Wagner, Wolfgang Part 1.

[17] J. Parajka, V. Naeimi, G. Bloschl, and J. Komma. Matching ers scatterometer based soil moisture patterns with simulations of a conceptual dual layer hydrologic model over austria. *Hydrology and Earth System Sciences*, 13(2):259–271, 2009. Parajka, J. Naeimi, V. Bloeschl, G. Komma, J.

[18] C. Rudiger, J. C. Calvet, C. Gruhier, T. R. H. Holmes, R. A. M. de Jeu, and W. Wagner. An intercomparison of ers-scat and amsr-e soil moisture observations with model simulations over france. *Journal of Hydrometeorology*, 10(2):431–447, 2009. Ruediger, Christoph Calvet, Jean-Christophe Gruhier, Claire Holmes, Thomas R. H. de Jeu, Richard A. M. Wagner, Wolfgang.

[19] K. Scipal. *Global soil moisture retrieval from ERS scatterometer data*. PhD thesis, Vienna University of Technology, Institute for Photogrammetry and Remote Sensing, 2002.

[20] K. Scipal, C. Scheffler, and W. Wagner. Soil moisture-runoff relation at the catchment scale as observed with coarse resolution microwave remote sensing. *Hydrology and Earth System Sciences*, 9(3):173–183, 2005.

[21] F. T. Ulaby, R. K. Moore, and A. K. Fung. *Microwave Remote Sensing: Active and Passive*, volume Volume 2: Radar Remote Sensing and Surface Scattering and Emission Theory. Reading, Massachusetts, Addison-Wesley, Advanced Book Program, 1982.

[22] W. Wagner, G. Lemoine, M. Borgeaud, and H. Rott. A study of vegetation cover effects on ers scatterometer data. *Ieee Transactions on Geoscience and Remote Sensing*, 37(2):938–948, 1999. Part 2.

[23] W. Wagner, G. Lemoine, and H. Rott. A method for estimating soil moisture from ers scatterometer and soil data. *Remote Sensing of Environment*, 70(2):191–207, 1999.

[24] W. Wagner, J. Noll, M. Borgeaud, and H. Rott. Monitoring soil moisture over the canadian prairies with the ers scatterometer. *Ieee Transactions on Geoscience and Remote Sensing*, 37(1):206–216, 1999. Part 1.

[25] W. Wagner and K. Scipal. Large-scale soil moisture mapping in western africa using the ers scatterometer. *Ieee Transactions on Geoscience and Remote Sensing*, 38(4):1777–1782, 2000. Part 2.

[26] W. Wagner, K. Scipal, C. Pathe, D. Gerten, W. Lucht, and B. Rudolf. Evaluation of the agreement between the first global remotely sensed soil moisture data with model and precipitation data. *Journal of Geophysical Research-Atmospheres*, 108(D19), 2003.

[27] Deming Zhao, Claudia Kuenzer, Congbin Fu, and Wolfgang Wagner. Evaluation of the ers scatterometer-derived soil water index to monitor water availability and precipitation distribution at three different scales in china. *Journal of Hydrometeorology*, 9(3):549–562, 2008.

Met Office
FitzRoy Road, Exeter
Devon, EX1 3PB
UK

Tel: 0870 900 0100
Fax: 0870 900 5050
enquiries@metoffice.gov.uk
www.metoffice.gov.uk